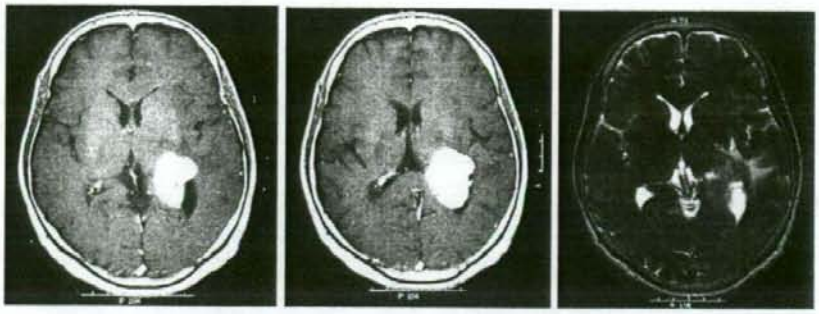

Fig. 1. Left and center: Preoperative gadolinium-enhanced T1-weighted MR images demonstrating a homogeneously enhanced mass at the left trigonal region, extending predominantly in the anterior direction. Right: A T2-weighted MR image showing moderate edema around the mass.

A parieto-occipital interhemispheric precuneus approach was chosen for removal of the mass. Lumbar spinal drainage was performed preoperatively. The patient was placed in a right upper semiprone position, and the head was maintained in a 3-point fixation device. The sagittal midline plane was rotated to lower the lesion side to gain gravity retraction. A left parieto-occipital craniotomy was performed extending beyond the superior sagittal sinus. The medial surface of the left cerebral hemisphere was retracted laterally, preserving bridging veins draining into the sagittal sinus. The left precuneus cortex was incised 1.5 cm long between the splenium and the parieto-occipital sulcus. The intraventricular tumor was reached by guidance of the frameless navigation system at a distance of 2 cm from the brain surface. Microscissors and potassium titanyl phosphate laser were used to debulk the tumor piecemeal from the medial to lateral portion. Vessels between the tumor and the choroid plexus were cauterized and interrupted. Finally, the most lateral portion of the tumor was dissected from the choroid plexus, and total removal was achieved. Histologic diagnosis of the tumor was a fibrous meningioma. Postoperative MRI demonstrated the avenue approaching the left trigone from the interhemispheric fissure and confirmed complete removal of the tumor (Fig. 2, left and right).

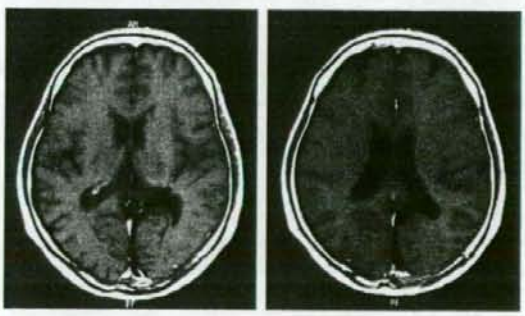

Fig. 2. Left and right: Postoperative gadolinium-enhanced T1-weighted images demonstrating the route approaching the left trigone from the interhemispheric fissure and confirming complete removal of the tumor.

Postoperative neurologic examination of the patient did not disclose any deficits of motor, speech, or visual functions; however, recent memory disturbance was recognized. She did not remember what she had done or heard several hours before. For example, she could not say what she had eaten at the last meal. Although memory disturbance gradually improved over the following 2 months, she still forgot half of the events that happened on the previous day. Three months postoperatively, the patient completely recovered memory function. The neurologic status has remained normal for 4 years.

## 3. Discussion

Using any surgical approach, callosotomy or corticotomy of normal brain territory is necessary to reach a trigonal tumor in the lateral ventricle. An appropriate approach should be selected to prevent neurologic sequelae such as visual field defect and higher brain dysfunctions, particularly on the dominant side. A variety of surgical approaches to the trigone have been described in past reports. For trigonal tumors of a dominant hemisphere, Kempe and Blaylock [8] recommended a transcallosal approach that decreased the frequency of postoperative seizures and risks of injury to the optic radiation. This approach, however, may cause a disconnection syndrome in right-handed patients with preexisting right homonymous hemianopia [11], and is not suitable for large tumors extending laterally [2]. Transcortical approaches that incise the inferior parietal or posterior temporal lobe often cause motor and speech deficits and damage to the optic radiation [2,12]. A paramedian parieto-occipital route is the most familiar approach to the trigone in the dominant hemisphere [2,4,12]. Although this approach theoretically can avoid injury to the optic radiation that runs inferolaterally to the trigone, postoperative visual field defects sometimes appear [7]. Other disadvantages of this approach are possible postoperative deficits of motor and language functions and difficulty in early access to the feeding vessels. Nakamura et al [12] reported that 7 of 13 patients with lateral ventricle meningiomas had cognitive and personality disturbance at the time of presentation, such

as memory disturbance, mental exhaustion, and dullness. After surgery via a posterior parieto-occipital transcortical approach, cognitive improvement was seen in 4 of 7 patients but remained the same in 3. None of the patients showed worsening or new development of memory disturbance.

A parieto-occipital interhemispheric precuneus approach was performed by Yasargil [13] and others [5,9]. Trigonal tumors are removed by this approach without direct injury to the optic radiation. For all its disadvantages such as deep and narrow working space and poor visualization of feeding arteries obscured by the tumor, this approach is thought to rarely cause impairment of higher brain functions in the dominant hemisphere [5,9]. Hussein [5] resected meningiomas of the trigonoatrial region in 8 patients using the interhemispheric transatrial (precuneus) approach. Most of the patients had preoperative neurologic symptoms including hemianopia, personality change, and increased intracranial pressure. Postoperatively, none of these patients experienced memory disturbance or worsening of preexisting symptoms.

Postoperative disturbance of recent memory developed in our patient, but fortunately, it disappeared in 3 months. One of the possible mechanisms of this deficit is dysfunction of the fornix due to surgical intervention. The anterior wall of the trigone is composed of the crus of fornix and the pulvinar, and the choroid plexus is located between them [6]. Unilateral transection of the fornix, even if it is performed on the nondominant side, causes severe memory impairment [3]. When the intraventricular meningioma enlarges, the normal ependymal layer disappears and the tumor adheres to the periventricular tissues [2]. In the present case, preoperative MRI demonstrated that the tumor extended predominantly in the anterior direction. Intraoperative manipulation around the attachment of the tumor might have injured a part of the crus of fornix resulting in the patient's postoperative symptom.

Another possible reason for the patient's memory deficit might be direct damage to the precuneus region. Based on studies in cognitive neuroscience, the precuneus has been recognized to play a role in retrieving visual, auditory, and episodic memory, regardless of dominancy of the brain hemisphere [1,10]. Fletcher et al concluded that the precuneus is a key part of the neural pathway of visual imagery occurring in conscious memory recall [1]. Krause et al [10] performed a PET scan to demonstrate that the precuneus is significantly activated not only during recall of words presenting tangible objects, but also during recall of abstract words. Although the detailed role of the precuneus remains unclear, surgeons should be reminded that there is a possibility that injury of this region may have some impact on memory function.

We think an interhemispheric precuneus approach is a useful alternative to trigonal tumors with few surgical complications. However, as seen in our case, postoperative memory disturbance can be one of the pitfalls after this procedure. Unfortunately, we missed a chance to test detailed memory functions of the patient. Careful evaluation of the patient's cognitive functions, including memory disturbance, should be recommended before and after surgery by this approach.

## References

[1] Fletcher PC, Frith CD, Baker SC, et al. The mind's eye. Precuneus activation in memory-related imagery. Neuroimage 1995;2:195-200.

[2] Fornari M, Savoiardo M, Morello G, et al. Meningioma of the lateral ventricles. Neuroradiological and surgical considerations in 18 cases. J Neurosurg 1981;54:64-74.

[3] Gaffan D, Gaffan EA. Amnesia in man following transection of the fornix. Brain 1991;114:2611-8.

[4] Guidetti B, Delfini R, Gagliardi FM, et al. Meningioma of the lateral ventricles. Clinical, neuroradiologic, and surgical considerations in 19 cases. Surg Neurol 1985;24:364-70.

[5] Hussein S. Operative management of the trigono-atrial lesion. [in German] Zentralbl Neurochir 1998;59:243-55.

[6] Ishii R, Suzuki Y, Watanabe A, et al. Gross total removal of gliomas in the pulvinar and correlative microsurgical anatomy. Neurol Med Chir (Tokyo) 2002;42:536-46.

[7] Jun CL, Nutik SL. Surgical approaches to intraventricular meningiomas of the trigone. Neurosurgery 1985;16:416-20.

[8] Kempe LG, Blaylock R. Lateral-trigonal intraventricular tumors. A new operative approach. Acta Neurochir 1976;35:233-42.

[9] Kinoshita A, Ito M, Yamanaka K, et al. Precuneus transcortical approach for intraventricular meningioma into the trigone of the dominant hemisphere. [in Japanese] CP Neurosurg 1998;8:891-4.

[10] Krause BJ, Schmidt D, Mottaghy FM, et al. Episodic retrieval activates the precuneus irrespective of the imagery content of word pair associates. A PET study. Brain 1999;122:255-63.

[11] Levin HS, Rose JE. Alexia without agraphia in a musician after transcallosal removal of a left intraventricular meningioma. Neurosurgery 1979;4:168-74.

[12] Nakamura M, Roser F, Bundschuh O, et al. Intraventricular meningiomas: a review of 16 cases with reference to the literature. Surg Neurol 2003;59:491-504.

[13] Yasargil MG. Parieto-occipital interhemispheric approach. In: Yasargil MG, editor. Microneurosurgery, vol. IVB. New York: Thieme; 1996. p. 56-7.

TECHNICAL NOTE

# Differential Diagnosis of the Infundibular Dilation and Aneurysm of Internal Carotid Artery: Assessment with Fusion Imaging of 3D MR Cisternography/Angiography

T. Satoh
M. Omi
C. Ohsako
K. Fujiwara
K. Tsuno
W. Sasahara
K. Onoda
K. Tokunaga
K. Sugiu
I. Date

**SUMMARY:** Fusion imaging of 3D MR cisternography/angiography was used for the assessment of the vascular bulging finding detected by MR angiography from the viewpoint of the outer wall configuration of the corresponding internal carotid artery depicted by MR cisternography. With a fusion image, useful information was obtained to distinguish an infundibular dilation and enlarged origin of the normal posterior communicating artery from an aneurysm. This imaging technique can be a feasible addition to a noninvasive screening of cerebrovascular lesions with MR angiography alone.

MR angiography is a noninvasive technique for vascular imaging and is thus widely used to screen for cerebrovascular lesions, including asymptomatic unruptured cerebral aneurysms.[1-3] Infundibular dilation is often detected at branching sites of the posterior communicating and anterior choroidal arteries from the internal carotid artery,[4-6] and this needs to be differentiated from an aneurysm. In this communication, we used a fusion imaging technique of 3D MR cisternography/angiography[7,8] to assess the vascular bulging finding detected by MR angiography from the viewpoint of the outer wall configuration of the corresponding internal carotid artery depicted by MR cisternography.

## Technique

### *MR Angiography Data Acquisition*

Patients with vascular bulging findings of the internal carotid artery detected at MR angiography underwent MR cisternography. MR angiography was performed with a clinical MR imager (Signa HiSpeed 1T; General Electric Healthcare, Milwaukee, Wisc) by using a 3D time-of-flight (TOF) sequence, spoiled gradient-recalled acquisition in the steady state. We used the following parameters: TR/TE, 35/4.0; number of excitations, 2; flip angle, 20°; matrix, 192 × 128; section thickness, 1.2 mm; section interval, 0.6 mm; field of view, 16 cm; without magnetization transfer contrast; zero-fill interpolation processing 2 times; 120 sections in total (2 slabs); overlap of 8 sections; and total of 104 overlapping source images acquired in 8 minutes 49 seconds. Volume data were transferred to an independent workstation with medical visualization software (Zio M900 Quadra; AMIN, Tokyo, Japan). Data were interpolated every 0.6 mm, and processed into 3D volume-rendering datasets. The 3D MR angiogram was rendered with a perspective volume-rendering algorithm by using an increasing curve starting with a threshold of 170–180 (0% opacity level) and up to 190–200 (100% opacity level, width 20), with a visual angle of 90°, and color-rendered in red.

### *MR Cisternography Data Acquisition*

MR cisternography was performed with the same scan baseline, and data were obtained by using a T2-weighted 3D fast spin-echo sequence. We used the following parameters: TR/TE, 4000/160; number of excitations, 1; echo train length, 128; bandwidth, 15.63 KHz; matrix, 256 × 256; section thickness, 0.6 mm; section interval, 0.6 mm; field of view, 16 cm. A total of 96 continuous source axial images were acquired in 13 minutes and 23 seconds. Data were interpolated every 0.6 mm and processed into 3D volume-rendering datasets. The 3D MR cisternogram was rendered with perspective volume-rendering algorithm by using an declining curve starting with a threshold of 390–450 (100% opacity level) and down to 410–470 (0% opacity level, width 20), with a visual angle of 90°, and color-rendered in blue.

### *Reconstruction of Fusion Images of 3D MRC and MRA*

A fusion image of 3D MR cisternography/angiography was reconstructed on a workstation by compositing 3D MR cisternography and its coordinated 3D MR angiography; each individual image was rendered from each volume-rendering dataset. To emphasize the vascular components, MR angiography-weighted fusion image was employed by overlapping 3D MR cisternogram (opacity level of 15%, in blue) and 3D MR angiogram (100% opacity level, in red). Total time required to produce the 3D MR cisternogram, 3D MR angiogram, and fusion image was approximately 30 seconds per image from postscanning.

Received August 9, 2005; accepted September 4.

From the Departments of Neurological Surgery (T.S., W.S.) and Diagnostic Radiology (M.O., C.O.), Ryofukai Satoh Neurosurgical Hospital, Fukuyama, Hiroshima, Japan; Department of Neurological Surgery (K.F., K.T.), Kosei General Hospital, Mihara, Hiroshima, Japan; and Department of Neurological Surgery (W.S., K.O., K.T., K.S., I.D.), Okayama University Postgraduate School of Medicine, Dentistry and Pharmaceutical Sciences, Okayama, Japan.

Presented in part at the 14th annual meeting of Japanese Society for Detection of Asymptomatic Brain Disease, July 1–2, 2005, Nagoya, Japan.

Address correspondence to Toru Satoh, MD, Department of Neurological Surgery, Ryofukai Satoh Neurosurgical Hospital, 5-23-23 Matsunaga, Fukuyama, Hiroshima, 729-0104, Japan.

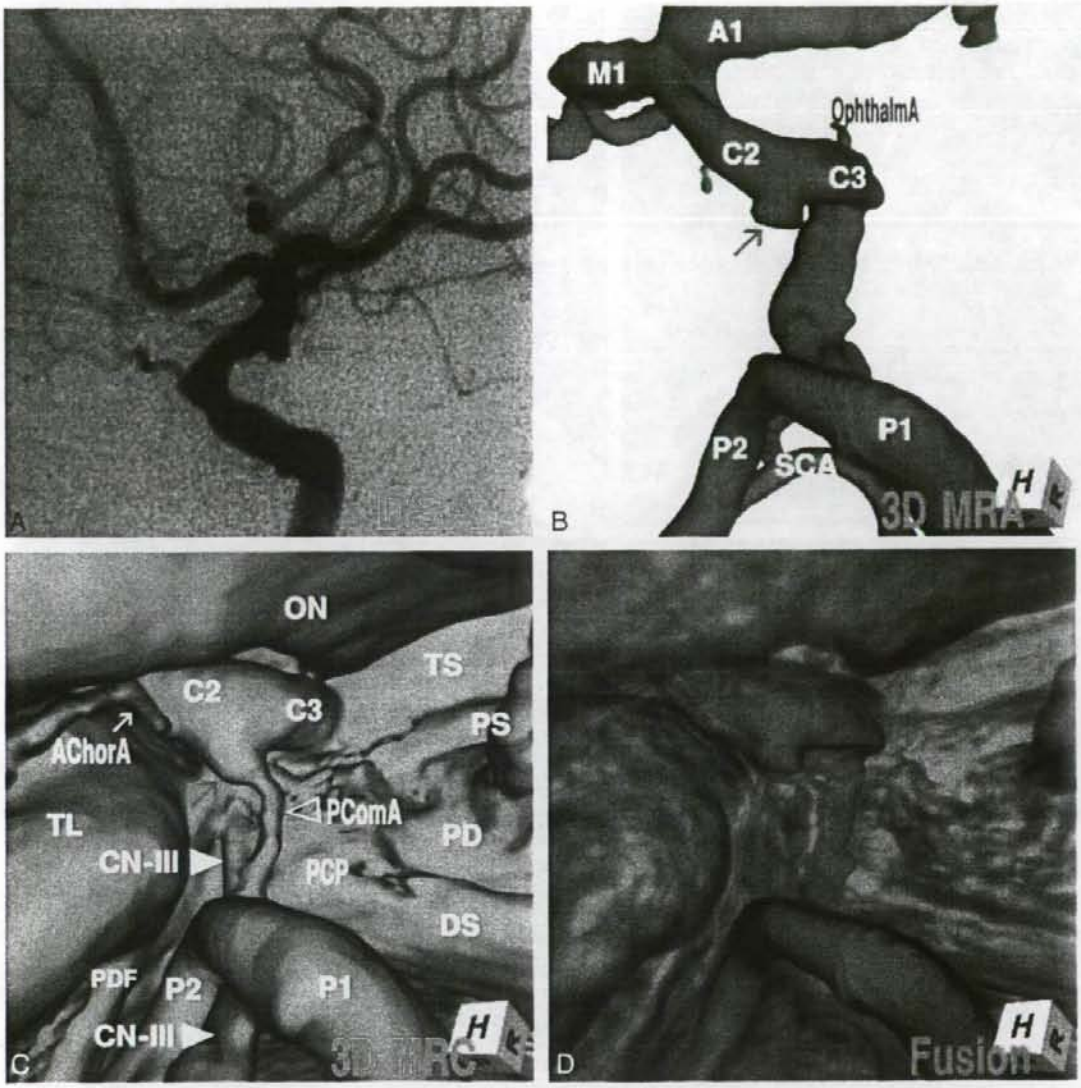


**Fig 1.** Case 1. Left infundibular dilation at the junction of the internal carotid artery–posterior communicating artery (adult type) in a 75-year-old woman.

*A*, Digital subtraction angiogram shows a round bulging (*arrow*) at the supraclinoid internal carotid artery.

*B*, 3D MR angiogram shows the trapezoid protrusion (*arrow*) at the supraclinoid internal carotid artery. A1, the first segment of the anterior cerebral artery; M1, the first segment of the middle cerebral artery; C2, the second segment of the internal carotid artery; C3, the third segment of the internal carotid artery; P1, the first segment of the posterior cerebral artery; P2, the second segment of the posterior cerebral artery; SCA, superior cerebellar artery.

*C*, 3D MR cisternogram, coordinated projection as to the 3D MR angiogram in *B*, shows an infundibular dilation (*arrow*) at the junction of the internal carotid artery-posterior communicating artery. A small posterior communicating artery arises at the apex. Intra- and juxtacisternal anatomic elements surrounding an infundibular dilation are visualized. ON, optic nerve; TS, tuberculum sellae; PS, pituitary stalk; PD, pituitary diaphragm; DS, dorsum sellae; PCP, posterior clinoid process; PComA, posterior communicating artery (▷); CN-III, oculomotor nerve (yellow arrow); PDF, petroclinoid dural fold.

*D*, Fusion image of the 3D MR angiography/cisternography shows the relationship of the bulging finding detected by the 3D MR angiography and its outer wall configuration depicted by the 3D MR cisternography.

## Illustrative Cases

### *Case 1: Left Infundibular Dilation at the Junction of the Internal Carotid Artery–Posterior Communicating Artery (Adult Type), a 75-Year-Old Woman*

The digital subtraction angiogram (Fig 1*A*), left lateral projection, showed a round protrusion (2.6-mm maximum diameter) at the posterior wall of the supraclinoid internal carotid artery. The 3D MR angiogram (Fig. 1*B*), right superoposterior projection, detected the trapezoid bulging extended posteriorly. The 3D MR cisternogram (Fig. 1*C*), coordinated projection as to the 3D MR angiogram in Fig 1*B*, depicted an infundibular dilation at the junction of the

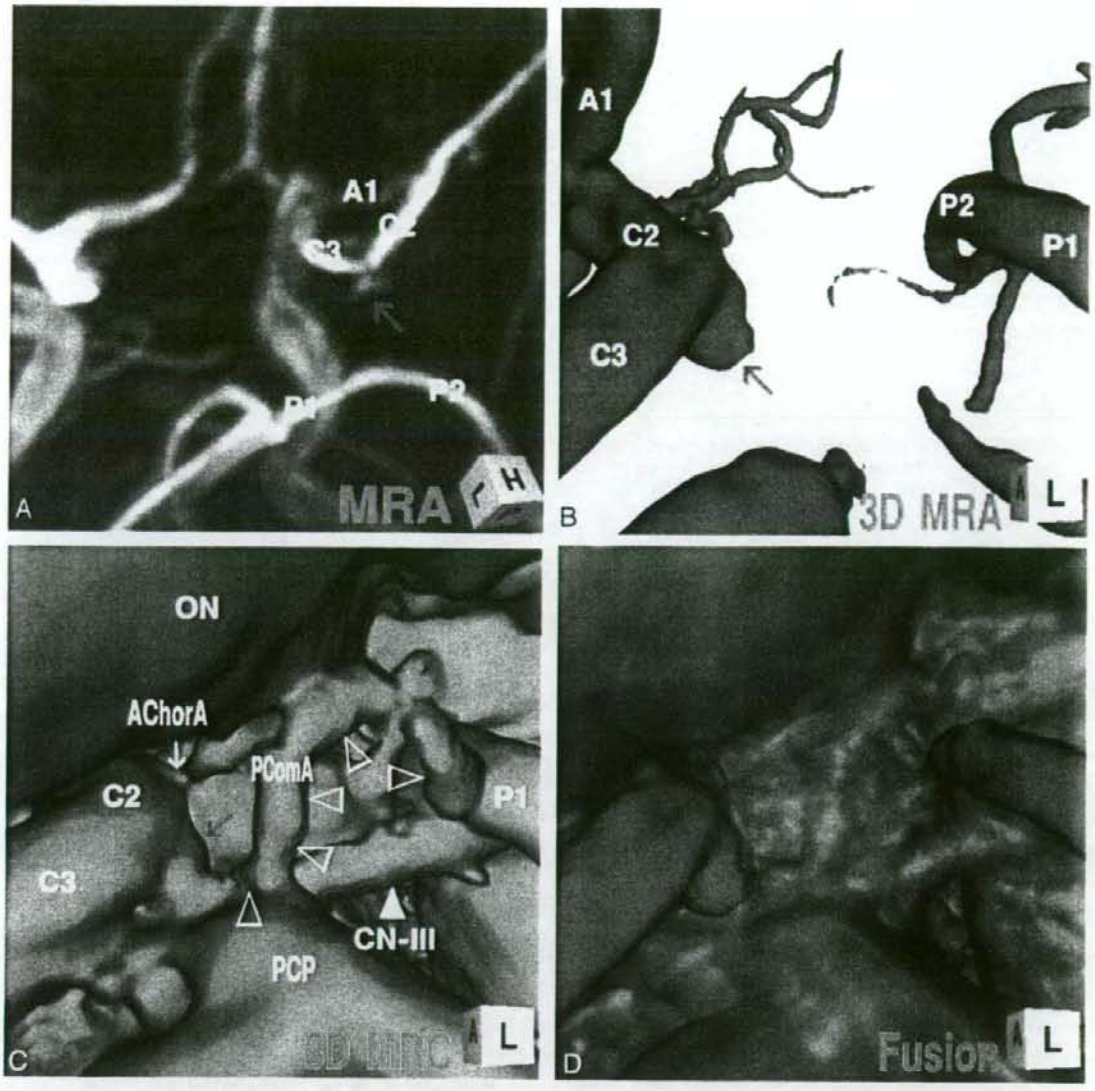


**Fig 2.** Case 2. Right infundibular dilation at the junction of the internal carotid artery–posterior communicating artery (fetal-type), in a 36-year-old woman.

*A*, Maximum intensity projection image of MR angiogram shows a trapezoidal bulging (*arrow*) at the posterior portion of the supraclinoid internal carotid artery.

*B*, 3D MR angiogram shows an aneurysm-like protrusion (*arrow*).

*C*, 3D MR cisternogram, coordinated projection as to the 3D MR angiogram *B*, shows an infundibular widening (*large arrow*) with a large posterior communicating artery (▷), bended at the posterior clinoid process and run tortuously to the posterior cerebral artery. ON, optic nerve; AChorA, anterior choroidal artery (*small arrow*); PComA (▷).

*D*, Fusion image of the 3D MR angiography/cisternography shows not an aneurysm but an infundibular dilation.

internal carotid artery–posterior communicating artery, but with a posterior communicating artery (adult-type) arising at the apex. Intra- and juxtacisternal anatomic elements surrounding an infundibular dilation including vessels, optic nerve, oculomotor nerve, posterior clinoid process, petroclinoid dural fold, and temporal lobe were depicted simultaneously. Fusion image of the 3D MR angiography/cisternography (*D*) clearly visualized the relationship of the bulging finding detected by the 3D MR angiography and its corresponding outer wall configuration depicted by the 3D MR cisternography.

### *Case 2: Right Infundibular Dilation at the Junction of the Internal Carotid Artery–Posterior Communicating Artery (Fetal Type), a 36-Year-Old Woman*

The maximum intensity projection image of MR angiogram (Fig 2*A*), left superoposterior projection, showed a trapezoid bulging (2.7-mm maximum diameter) at the posterior portion of the supraclinoid internal carotid artery. The 3D MR angiogram (Fig. 2*B*), left anterior projection, showed an aneurysm-like protrusion with an irregular dome tip. The 3D MR cisternogram (Fig. 2*C*), coordinated projection as to the 3D MR angiogram in Fig 2*B*, depicted an infundibular widening

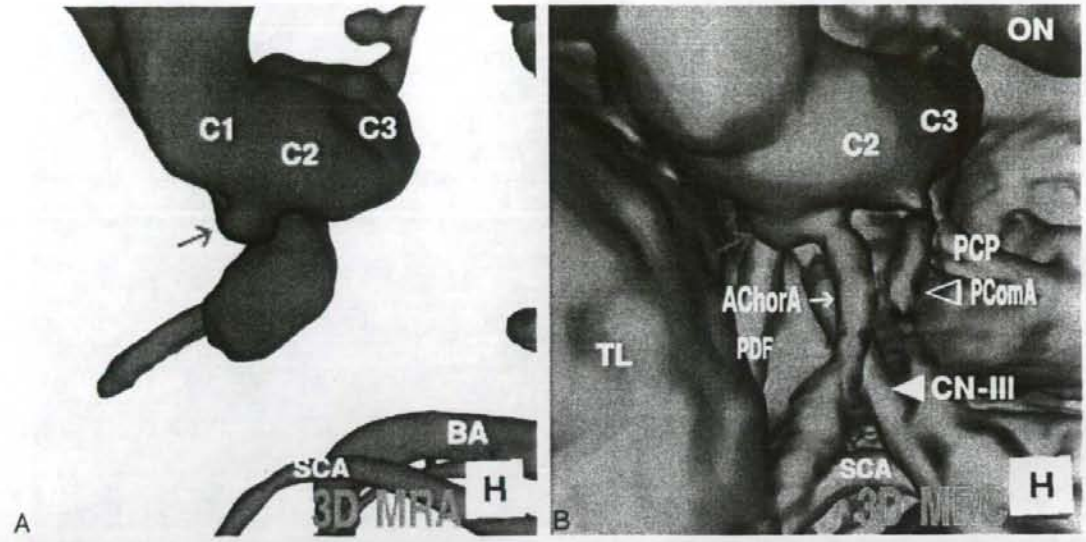


**Fig 3.** Case 3. Left infundibular dilation at the junction of the internal carotid artery–anterior choroidal artery, in a 69-year-old woman.

*A*, 3D MR angiogram shows an aneurysm-like trapezoid bulging (*arrow*). C1, the first segment of the internal carotid artery; BA, basilar artery.

*B*, 3D MR cisternogram, coordinated projection as to the 3D MR angiogram in *A*, shows an infundibular dilation (*large arrow*) at the junction of the anterior choroidal artery (*small arrow*). PComA (▷); CN-III ([GRAPHIC]); TL, temporal lobe.

*C*, Fusion image of the 3D MR angiography/cisternography shows an infundibular dilation at the junction of an anterior choroidal artery.

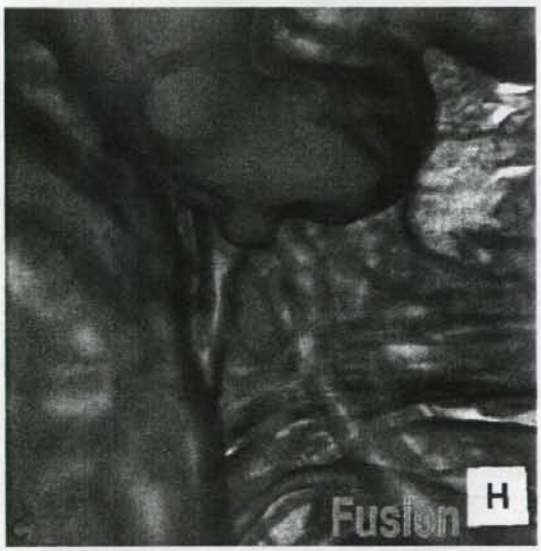


with a large posterior communicating artery (fetal type), bent at the right corner of the posterior clinoid process and run tortuously up and down to the posterior cerebral artery. With a fusion image of the 3D MR angiography/cisternography (Fig. 2*D*) the bulging finding of 3D MR angiography was discerned not an aneurysm but an infundibular dilation.

### *Case 3: Left Infundibular Dilation at the Junction of the Internal Carotid Artery–Anterior Choroidal Artery, a 69-Year-Old-Woman*

The 3D MR angiogram (Fig 3*A*), superoinferior projection, showed an aneurysm-like trapezoid bulging (2.7-mm maximum diameter) at the posterior portion of the supraclinoid internal carotid artery. The 3D MR cisternogram (Fig. 3*B*), coordinated projection as to the 3D MR angiogram in Fig 3*A*, depicted an infundibular dilation not at the junction of the posterior communicating artery but at the anterior choroidal artery. The anterior choroidal artery arose at the side of the infundibular dilation and ran posterolaterally to the choroidal fissure. The fusion image of the 3D MR angiography/cisternography (Fig. 3*C*) discriminated an infundibular dilation from an anterior choroidal artery aneurysm.

### *Case 4: Right Infundibular Dilation at the Junction of the Internal Carotid Artery–Posterior Communicating Artery (Fetal Type), Misdiagnosed as an Aneurysm and Treated Surgically, a 44-Year-Old Woman*

This patient was misdiagnosed and operated on for an unruptured internal carotid–posterior communicating artery aneurysm with a bleb. Operative findings disclosed a simple infundibular widening at the origin of a large posterior communicating artery, and coating of the protrusive portion was performed in the operation. The MR angiography/cisternography was examined postoperatively. The 3D MR angiogram (Fig 4*A*), superoinferior projection, showed an aneurysm-like protrusion with a round dome and a conical bleblike elongation (3.2-mm maximum diameter) at the posteromedial portion of the supraclinoid internal carotid artery. The 3D MR cisternogram (Fig. 4*B*), coordinated projection as to the 3D MR angiogram in Fig 4*A*, depicted an infundibular dilation with a large posterior communicating artery (fetal type). The posterior communicating artery was bent at the right lateral edge of the posterior clinoid process and run posteriorly to the posterior cerebral artery. Fusion image of the 3D MR angiography/cisternography (Fig. 4*C*) visualized the anatomic relationship of an aneurysm-like complex to a large posterior

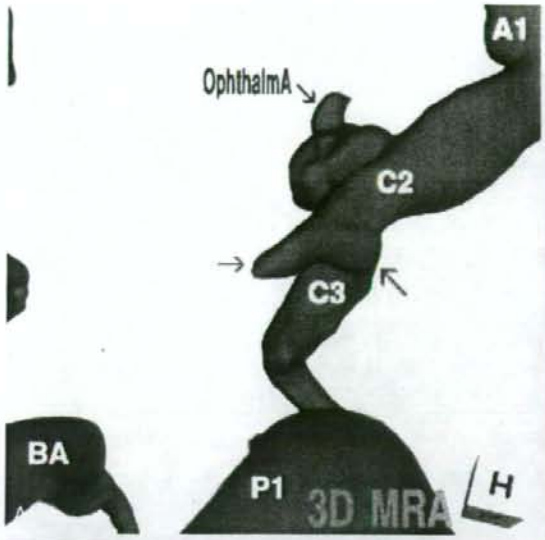


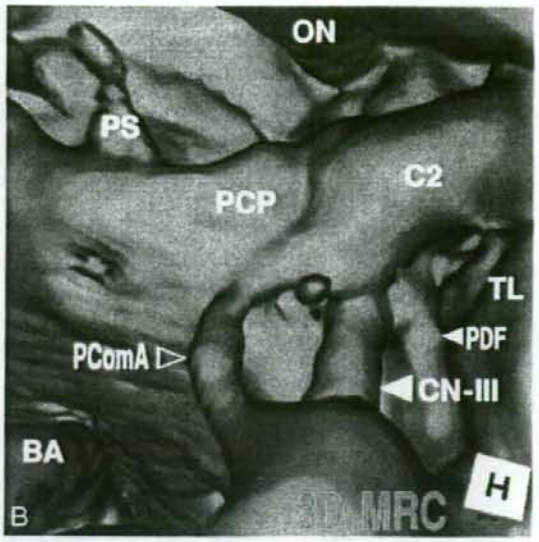


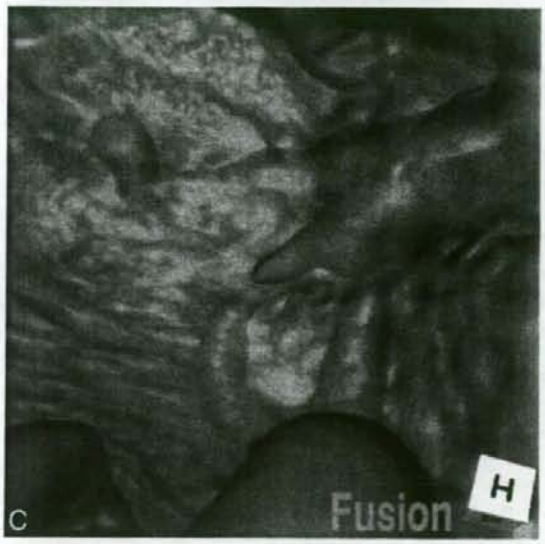


**Fig 4.** Case 4. Right infundibular dilation at the junction of the internal carotid artery–posterior communicating artery (fetal type), misdiagnosed as an aneurysm and treated surgically, in a 44-year-old woman.

*A*, 3D MR angiogram shows an aneurysm-like protrusion (*large arrow*) and a conical blebliike elongation (*small arrow*).

*B*, 3D MR cisternogram, coordinated projection as to the 3D MR angiogram in *A*, shows an infundibular dilation (*arrow*) with a large posterior communicating artery. PDF (*small arrow*); CN-III (*large arrow*); PComA (▷).

*C*, Fusion image of the 3D MR angiography/cisternography shows the anatomic relationship of an aneurysm-like complex to a large posterior communicating artery, and indicating not an aneurysm but an infundibular dilation.

communicating artery; thus the bulging portion was diagnosed as not an aneurysm with a bleb but an infundibular dilation accompanying a large posterior communicating artery.

### *Case 5: Left Internal Carotid Artery–Posterior Communicating Artery Aneurysm, a 66-Year-Old Woman*

The 3D MR angiogram (Fig 5*A*), right superoposterior projection, showed an aneurysm with an irregular dome (3.9 mm in the maximum diameter) at the junction of the internal carotid artery–posterior communicating artery. The 3D MR cisternogram (*B*), coordinated projection to the 3D MR angiogram in Fig 5*A*, depicted an aneurysm and a large posterior communicating artery (fetal type). The dome extended inferoposteromedially toward the left lateral edge of the posterior clinoid process and the left oculomotor nerve. Fusion image of the 3D MR angiography/cisternography (Fig. 5*C*) clearly visualized the aneurysm complex in relation to its perianeurysmal environment.

## Discussion

With use of MR angiography for screening of cerebrovascular lesions, vascular bulging is frequently observed at the supraclinoid portion of the internal carotid artery.[2,9,10] Infundibular dilation most often affects the origin of the posterior communicating artery at its junction of the internal carotid artery. Incidence of infundibular dilation detected by angiography or at autopsy ranges from 7% to 25%, and increases with age.[4-6] Angiographic criteria for infundibular dilation include round or conical in shape, <3 mm in the maximum diameter, without aneurysmal neck, and with a posterior communicating artery arising from its apex.[5] Angiographic findings for this lesion, however, are difficult to interpret, and it is sometimes misdiagnosed and treated as an aneurysm.[9,10] In particular, when the posterior communicating artery does not filled well or appears very small, and when the anatomic relationship of the protrusion to the internal carotid artery is not clearly depicted, it is difficult to distinguish an infundibular dilation and enlarged origin of the normal posterior communicating artery from an aneurysm.[9-12]

MR angiography obtained by 3D TOF sequence represents not the luminal morphology as shown by angiography and CT angiography,[13,14] but inflow effect related mainly to peak inflow velocity within the vessel lumen during the data acquisi-

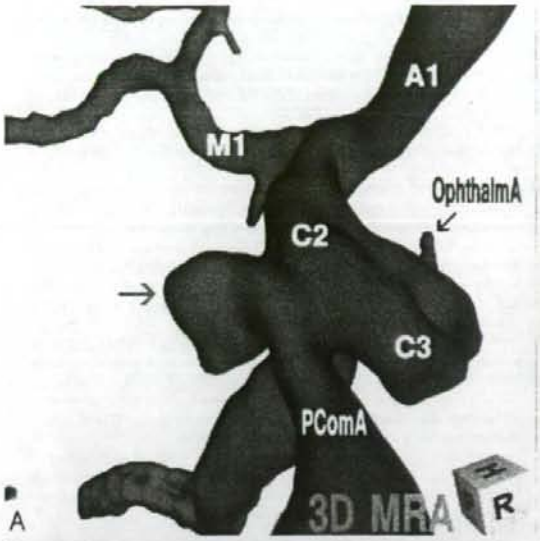


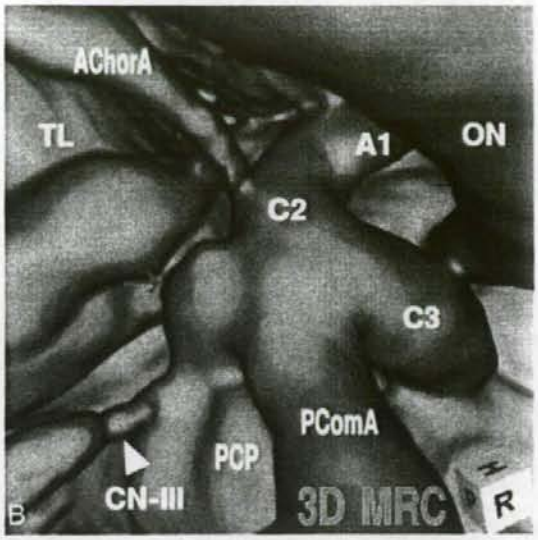


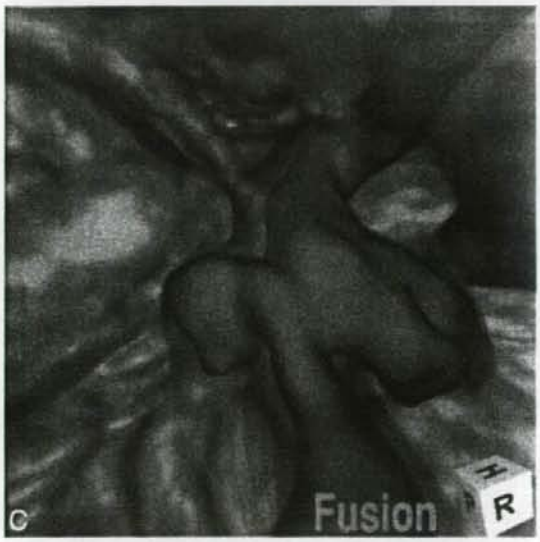


**Fig 5.** Case 5. Left internal carotid artery–posterior communicating artery aneurysm, in a 66-year-old woman.

*A*, 3D MR angiogram shows an aneurysm with an irregular dome (*arrow*).

*B*, 3D MR cisternogram, coordinated projection as to the 3D MR angiogram in *A*, shows an aneurysm (*arrow*) and a large posterior communicating artery. AChorA, anterior choroidal artery; CN-III (*arrow*).

*C*, Fusion image of the 3D MR angiography/cisternography shows the aneurysm complex in relation to its perianeurysmal environment.

tion process.[1,3] The magnitude of signal intensity of MR angiography is complicated and affected by several factors. Loss of signals occurs from spin saturation phenomenon due to slow flow, phase dispersion due to complex and disturbed flow conditions, and susceptibility or partial volume effects.[3] Decrease in signal intensity and inhomogeneous signal intensity distribution are often observed within an aneurysm and at the origin of the branching site of vessels. In addition, when the flow condition within the posterior communicating artery varies in complexity according to the directions of collateral flow in the circle of Willis,[15] inflow effect within the vessels may decrease, and this may result in poor visualization of the posterior communicating artery.

In contrast, MR cisternography depicts the vascular structures with profoundly low signal intensity, and cranial nerves and brain parenchyma with moderately low signal intensity; outer borderline of intracisternal anatomic elements is well demarcated by the profoundly hyperintense adjacent subarachnoid CSF.[7,8,16] 3D reconstruction of volume data acquired by MR cisternography can depict the morphologically fine outer wall configuration of the vessels in relation to the surrounding intra- and juxtacisternal structures.[7,8]

By using a fusion imaging technique of 3D MR cisternography/angiography, vascular structure of 3D MR cisternography and 3D MR angiography is composed in a single image.[7,8] With a 3D MR angiography alone, it may be difficult to depict the hypoplastic or small size (adult-type) posterior communicating artery associated with an infundibular dilation. In case of the well-developed (fetal-type) posterior communication artery but with a bended and tortuous running course, the whole shape of the vessel may not be shown owing to a decrease in inflow effect within a vessel. In contrast, 3D MR cisternography can depict the vascular contour unrelated to the intraluminal flow conditions; however, the extent of cisternographic view is limited primarily within a cisternal space and complicated by the nonvascular elements in the intra- and juxtacisternal space. With a fusion imaging technique of 3D MR cisternography/angiography, vascular structures depicted on the 3D MR cisternogram can be discriminated by referencing the coordinated 3D MR angiogram. Vascular bulging related to inflow effect detected by MR angiography may be assessed from the viewpoint of the outer wall configuration of the corresponding internal carotid artery by overlapping the coordinated MR cisternogram.

In conclusion, when a vascular bulging of the internal carotid artery is detected by MR angiography, assessment with a fusion imaging technique of 3D MR cisternography/angiogra-

phy may provide useful information to distinguish an infundibular dilation and enlarged origin of the normal posterior communicating artery from an aneurysm. This imaging technique can be a feasible addition to a noninvasive screening of cerebrovascular lesions with MR angiography alone.

## References


1. Adams WM, Laitt RD, Jackson A. **The role of MR angiography in the pretreatment assessment of intracranial aneurysms: a comparative study.** *AJNR Am J Neuroradiol* 2000;21:1618–28
2. Okahara M, Kiyosue H, Yamashita M. **Diagnostic accuracy of magnetic resonance angiography for cerebral aneurysms in correlation with 3D-digital subtraction angiographic images. a study of 133 aneurysms.** *Stroke* 2002;33:1803–808
3. Satoh T, Onoda K, Tsuchimoto S. **Visualization of intraaneurysmal flow patterns with transluminal flow images of 3D MR angiograms in conjunction with aneurysmal configurations.** *AJNR Am J Neuroradiol* 2003;24:1436–45
4. Salyzman GF. **Infundibular widening of the posterior communicating artery studied by carotid angiography.** *Acta Radiol* 1959;51:415–21
5. Taveras LM, Wood EH. **Diagnostic Neuroradiology.** 2nd ed. Baltimore, Williams & Wilkins, 1976, pp584–87
6. Ebina K, Ohkuma H, Iwabuchi T. **An angiographic study of incidence and morphology of infundibular dilation of the posterior communicating artery.** *Neuroradiology* 28 1986;28:23–29
7. Satoh T, Omi M, Ohsako C, et al. **Visualization of aneurysmal contours and perianeurysmal environment with conventional and transparent 3D MR cisternography.** *AJNR Am J Neuroradiol* 2005;26:313–18
8. Satoh T, Omi M, Ohsako C, et al. **Influence of perianeurysmal environment on the deformation and bleb formation of the unruptured cerebral aneurysm. Assessment with fusion imaging of 3D MR cisternography and 3D MR angiography.** *AJNR Am J Neuroradiol* 2005;26:2010–18
9. Endo S, Furuichi S, Takabe, et al. **Clinical study of enlarged infundibular dilation of the origin of the posterior communicating artery.** *J Neurosurg* 1995;83: 421–25
10. Kubota T, Niwa J, Tanigawara T, et al. **Differential diagnosis between aneurysm and infundibular dilation in the IC-PC region with 3D-CTA.** *No Shinkei Geka (Tokyo)* 2000;28:31–39 [in Japanese with English abstract]
11. Epstein F, Ransohoff J, Budzilovich GN. **The clinical significance of junctional dilation of the posterior communicating artery.** *J Neurosurg* 1970;33:529–31
12. Marshman LAG, Ward PJ, Walter PH, et al. **The progression of an infundibulum to aneurysm formation and rupture: case report and literature review.** *Neurosurgery* 1998;43:1445–49
13. Satoh T. **Transluminal imaging with perspective volume rendering of computed tomographic angiography for the delineation of cerebral aneurysms.** *Neurol Med Chir (Tokyo)* 2001;41:425–30
14. Satoh T, Onoda K, Tsuchimoto S. **Intra-operative evaluation on aneurysmal architecture. Comparative study with transluminal imaging of 3D MR and CT angiograms.** *AJNR Am J Neuroradiol* 2003;24:1975–81
15. Hartkamp MJ, van der Grond J, van Everdingen KJ. **Circle of willis collateral flow investigated by magnetic resonance angiography.** *Stroke* 1999;30:2671–78
16. Rubinstein D, Sandberg EJ, Breeze RE, et al. **T2-weighted three-dimensional turbo spin-echo MR of intracranial aneurysms.** *AJNR Am J Neuroradiol* 1997; 18:1939–43

available at www.sciencedirect.com

SCIENCE DIRECT®

www.elsevier.com/locate/brainres

BRAIN RESEARCH

Research Report

# Control of dopamine-secretion by Tet-Off system in an in vivo model of parkinsonian rat

*Kazuki Kobayashi, Takao Yasuhara*, Takashi Agari, Kenichiro Muraoka, Masahiro Kameda, wen Ji Yuan, Hitoshi Hayase, Toshihiro Matsui, Yasuyuki Miyoshi, Tetsuro Shingo, Isao Date*

*Department of Neurological Surgery, Okayama University Graduate School of Medicine, Dentistry, and Pharmaceutical Science, Okayama, Japan*

ARTICLE INFO

*Article history:*
Accepted 16 April 2006
Available online 27 June 2006

*Keywords:*
Cell therapy
Cerebrospinal fluid
Dopamine
Encapsulation
Parkinson's disease
Rat
Tet-Off system

ABSTRACT

We established a PC12 cell line (PC12TH Tet-Off) in which human tyrosine hydroxylase (TH) expression can be negatively controlled by Doxycycline (Dox). First, dopamine (DA)-secretion from PC12TH Tet-Off cells was controlled by Dox-administration in a dose-responsive manner ranging from 0 to 100 ng/ml for 70 days in vitro. Furthermore, Parkinson's disease model of rats receiving encapsulated PC12TH Tet-Off cells displayed a significant decrease of dopamine concentration in the cerebrospinal fluid (CSF) and increase of the number of apomorphine-induced rotations by Dox-administration, as compared to transplanted rats without Dox-administration, although the significant decrease of the reduction ratio of DA concentration in the CSF with Dox-administration was recognized over time. At 2 months post-implantation, concentration of dopamine in the implanted striatum and from the retrieved capsules demonstrated that the control of DA-secretion could be partially achieved for 2 months in vivo. Our results support both the value of cell therapy using Tet-Off system and the technique of encapsulation might be a feasible option for Parkinson's disease especially in resolving the problem of dopamine oversupply in the future, although a more efficient way to control DA-secretion with quicker regulation and much titration of dose should be explored before clinical application.



## 1. Introduction

The major pathology of Parkinson's disease (PD) is neurodegeneration of the dopamine-producing nigrostriatal system (Dawson and Dawson, 2002). Dopamine replacement therapy (DRT) was first established as a therapeutic modality for PD. However, patients with DRT for a long time often develop both dyskinesia and wearing-off (Nutt et al., 2002) with impairment of the synaptic dopamine (DA) metabolism in the putamen (Rajput et al., 2004). In recent years, cell therapy using fetal nigral cells (Freed et al., 2001; Olanow et al., 2003) was also reported to display a certain therapeutic effects on PD patients with significant effectiveness in the younger but sometimes induce dyskinesia in some severely staged PD patients. Positron emission tomography revealed that $^{18}$F fluorodopa uptake in the putamen significantly increased in the patients developing persistent dyskinesia (Ma et al., 2002). Thus, dyskinesia induced by DRT or fetal nigral cell transplantation might be certainly associated with oversupply of dopamine in a localized area. In this study, we demonstrated doxycycline

* *Corresponding author*. Fax: +81 86 227 0191.
E-mail address: tyasu37@cc.okayama-u.ac.jp (T. Yasuhara).

0006-8993/$ – see front matter © 2006 Elsevier B.V. All rights reserved.
doi:10.1016/j.brainres.2006.04.078

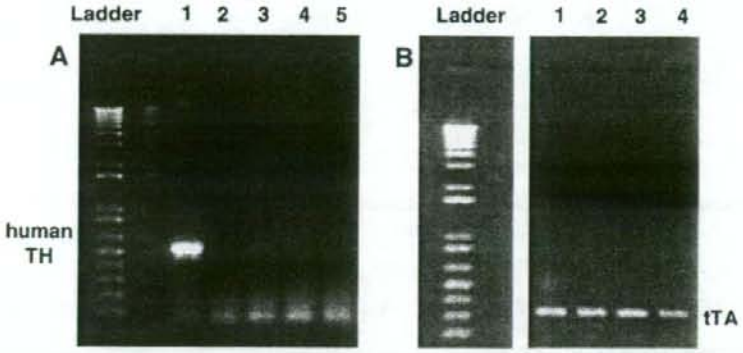


**Fig. 1 – RT-PCR revealed the reduction of human TH-expression of PC12TH Tet-Off cells by Dox-administration in vitro. (A) RT-PCR of hTH revealed the expression of hTH RNA from the PC12TH Tet-Off cells without Dox-administration (lane 3) and the reduced expression from cells with Dox-administration (lane 2). The expression of hTH was not recognized in PC12 Tet-Off Control cells with or without Dox-administration (lanes 4 and 5). Lane 1 was shown as a positive control using pTRE2hygTH1, plasmid carrying hTH gene. (B) Expression of Tet transactivator (tTA) RNA from PC12TH Tet-Off and PC12 Tet-Off Control cells with or without Dox-administration was recognized equally likely. Lanes 1 and 2: PC12TH Tet-Off cells with and without Dox-administration. Lanes 3 and 4: PC12 Tet-Off Control cells with and without Dox-administration.**

(Dox)-controlled expression of human tyrosine hydroxylase (hTH) with encapsulated cell transplantation with which we can use safely genetically engineered xenogeneic graft in an in vivo model of PD. These technologies can be used for dose control of neurotransmitter like dopamine or growth factor like vascular endothelial growth factor (VEGF), both of which might cause deteriorated outcomes with inappropriate dose administration (Yasuhara et al., 2005b). Furthermore, critical problems like tumorigenesis by transplanted cells might be prevented using cells encoded suicide gene in advance (Bondanza et al., 2005). The control of DA-secretion from the outside like this study might reduce the side effects of DRT upon PD patients and diminish the burden of PD patients suffering from severe dyskinesia induced by DRT.

## 2. Results

### 2.1. *Dox-controlled TH-expression in vitro*

The expressions of TH and tTA of PC12TH Tet-Off cells without Dox-administration were recognized by RT-PCR, and the TH-expression of PC12TH Tet-Off cells cultured with 1-week Dox-administration reduced remarkably (Fig. 1). The amount of LD and DA-secretion from cultured PC12TH Tet-Off, PC12 Tet-Off Control, PC12, and BHK cells were as follows: LD-secretion were 470 ± 8.4, 102 ± 4.0, 96 ± 4.2, and 0 ng/$10^6$ cells/day and DA-secretion was 56 ± 2.5, 16 ± 0.8, 9.5 ± 0.6, and 0 ng/$10^6$ cells/day, respectively. In addition, the amount of LD and DA-secretion from the 4 kinds of capsule at 2 weeks post-encapsulation was almost the same as each non-encapsulated $10^6$ cells (LD: 481 ± 13.8, 102 ± 6.8, 91.5 ± 5.7, and 0, DA: 57.3 ± 3.9, 15.6 ± 2.1, 9.2 ± 1.1, and 0 ng/$10^6$ cells/day, respectively). Dox-administration for 1 week (10–1000 ng/ml) was considered to reduce TH-expression of encapsulated PC12TH Tet-Off cells, and subsequently LD and DA-secretion significantly decreased in a dose-responsive manner from 0 to

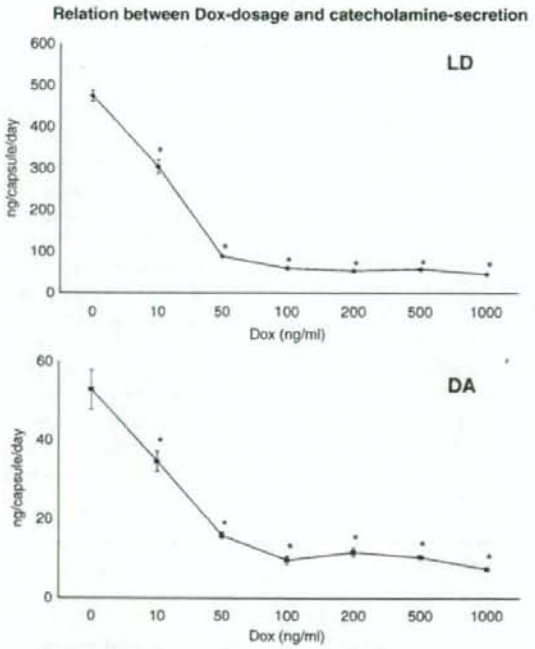


**Fig. 2 – Relation between the dose of Dox-administration and catecholamine-secretion from PC12TH Tet-Off cells in vitro. DA and LD-secretion from PC12TH Tet-Off cells was reduced by Dox-administration for 1 week in a dose-responsive manner ranging from 0 to 100 ng/ml. The degree of reduction of DA and LD-secretion with 100 ng/ml of Dox-administration was almost the same as with 1000 ng/ml. Data are shown as mean values ± SE expressed as ng/capsule/day. $n = 4$ in each group. *$P$'s < 0.01 vs. DA and LD-secretion from PC12TH Tet-Off capsule without Dox-administration by post hoc Scheffe's test.**

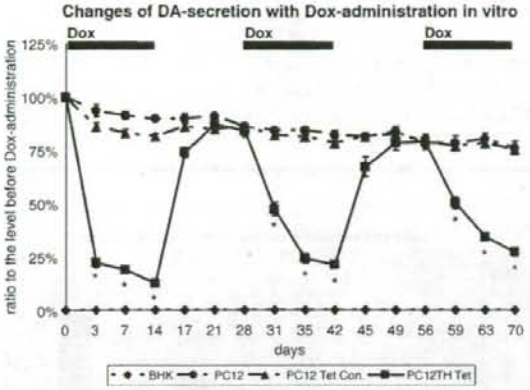


**Fig. 3 – Changes of DA-secretion from encapsulated cells with or without Dox-administration in vitro. DA-secretion from encapsulated PC12TH Tet-Off cells was clearly controlled by Dox-administration. However, at 1 week after the initiation of the second and third Dox-administration (at day 35 and 63), DA-secretion decreased to 24 ± 2.3 and 34 ± 1.9%, suggesting that the control of DA-secretion became slightly less effective with significant differences. Data are shown as mean values ± SE expressed as percentages of DA-secretion before Dox-administration (at day 0). PC12 Tet Con.; PC12 Tet-Off Control cells. $n = 6$ in each group. *$P$'s < 0.01 vs. DA-secretion from PC12TH Tet-Off capsule before Dox-administration by post hoc Scheffe's test.**

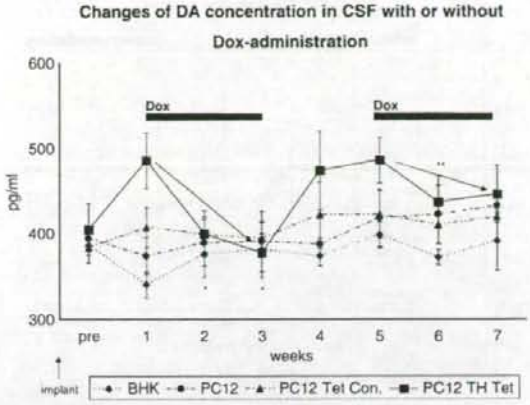


**Fig. 5 – Changes of DA concentration in the CSF of rats receiving encapsulated cell transplantation with or without Dox-administration. DA concentration in the CSF of rats receiving encapsulated PC12TH Tet-Off cells was clearly controlled by Dox-administration for the initial month. However, the second Dox-administration showed less reduction of DA concentration. Data are shown as mean values ± SE expressed as DA concentration in the CSF. PC12 Tet Con.; PC12 Tet-Off Control cells. $n = 8$ in PC12TH Tet-Off and PC12 Tet-Off Control groups. $n = 5$ in PC12 and BHK groups. *$P$'s < 0.05 vs. DA concentration in the CSF of rats receiving PC12 TH Tet-Off capsule before Dox-administration by post hoc Scheffe's test. **$P$ < 0.05 vs. the reduced ratio of DA concentration in the CSF from 1 to 3 weeks with the first Dox-administration. Arrow indicates the reduced ratio from 1 to 3 and 5 to 7 weeks.**

100 ng/ml for 70 days in vitro (DA: 52.8, 34.6, 15.8, and 9.6, DOPA: 474, 304, 88.6, and 59.6 ng/capsule/day with 0, 10, 50, 100 ng/ml of Dox, respectively), compared to that without Dox-administration (Fig. 2: DA; $F_{6,28} = 114.3$, $P < 0.0001$, LD; $F_{6,28} = 67.3$, $P < 0.0001$). Next, control of DA-secretion from the capsule in vitro with or without Dox-administration was confirmed for 3 months. After Dox-administration for 3 days, LD and DA-secretion from encapsulated PC12TH Tet-Off cells

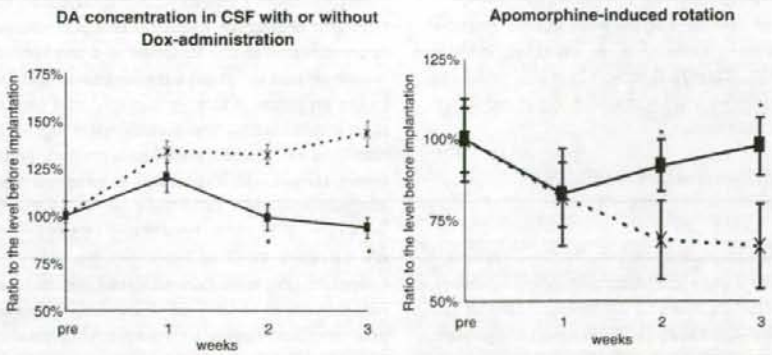


**Fig. 4 – Effects of Dox-administration upon DA concentration in the CSF and the number of apomorphine-induced rotation of 6-OHDA lesioned rats receiving PC12TH Tet-Off capsule in vivo. Dox-administration decreased DA concentration in the CSF and increased the number of apomorphine-induced rotation of 6-OHDA lesioned rats receiving PC12TH Tet-Off capsule after Dox-administration (solid line), compared to rats without Dox-administration (dotted line). Pre: before transplantation, 2-week Dox-administration was started at 1 week post-transplantation in the relevant rats. CSF: $n = 8$ in each group. *$P$'s < 0.05 vs. DA concentration of rats receiving PC12TH Tet-Off capsule without Dox-administration; Rotation number: $n = 12$ in each group. *$P$'s < 0.05 vs. rotation number of rats receiving PC12TH Tet-Off capsule without Dox-administration.**

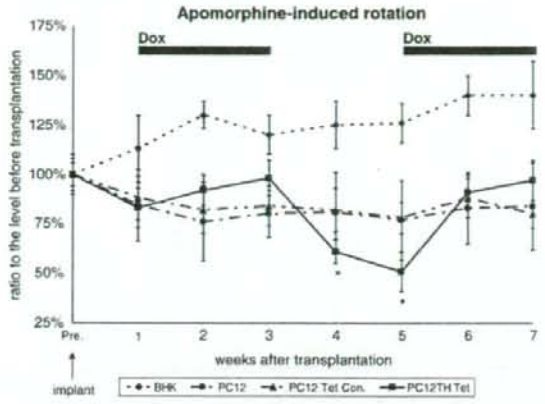


**Fig. 6 – Changes of the number of apomorphine-induced rotations of rats receiving encapsulated cell transplantation with or without Dox-administration. The number of apomorphine-induced rotations of rats receiving encapsulated PC12TH Tet-Off cells increased with Dox-administration and decreased with the discontinuation of Dox-administration. The rotational number of rats receiving BHK capsule, from which no catecholamine was secreted, was higher than that of rats in the other groups, which received catecholamine-secreting capsule. Data are shown as mean values ± SE expressed as percentages of the number before capsule implantation. PC12 Tet Con.; PC12 Tet-Off Control cells. $n = 14$ in PC12TH Tet-Off and PC12 Tet-Off Control groups, $n = 10$ in PC12 and BHK groups. *$P < 0.05$ vs. the number before Dox-administration by post hoc Scheffe's test.**

was reduced to 33 ± 1.2 and 22 ± 2.0% of the level before Dox-administration. Dox-administration was continued for 2 weeks and then, LD and DA-secretion increased to 81.3 ± 4.3 and 74.0 ± 2.3% at 3 days after discontinuation of Dox-administration. The control of DA-secretion could be achieved for over 70 days in vitro, although the control became slightly less efficient over time (Fig. 3, PC12TH Tet-Off; $F_{15,80} = 124.3$, $P < 0.0001$). Catecholamine-secretion from the other 3 kinds of encapsulated cells showed a slight reduction without significance differences.

### 2.2. *Dox-controlled TH-expression in vivo*

#### 2.2.1. *Body weight*

The procedure of capsule implantation resulted in a transient body weight loss (– 3% at 3 days post-implantation); however, there were no statistically significant differences among the PC12TH Tet-Off, PC12 Tet-Off Control, PC12, and BHK groups. Dox-administration also showed no significant loss in body weight.

#### 2.2.2. *DA assay in cerebrospinal fluid*

DA concentration in the CSF of rats with or without lesions was 400 ± 12.2 or 616 ± 26.2 pg/ml at 4 weeks after 6-OHDA lesions, exhibiting significant differences. After Dox-administration for 1 and 2 weeks, DA concentration in the CSF of rats receiving PC12TH Tet-Off capsule implantation significantly reduced to 400 ± 27.1 and 378 ± 22.3 pg/ml, compared to DA concentration without Dox-administration, 521 ± 19.8 and 565 ± 26 pg/ml (Fig. 4, left). Then, with 1-week discontinuation of Dox-administration, DA concentration in the CSF recovered to 473 ± 46.2 pg/ml (Fig. 5: PC12TH Tet-Off; $F_{7,104} = 7.89$, $P < 0.0001$). Thereafter, DA concentration in the CSF correlated

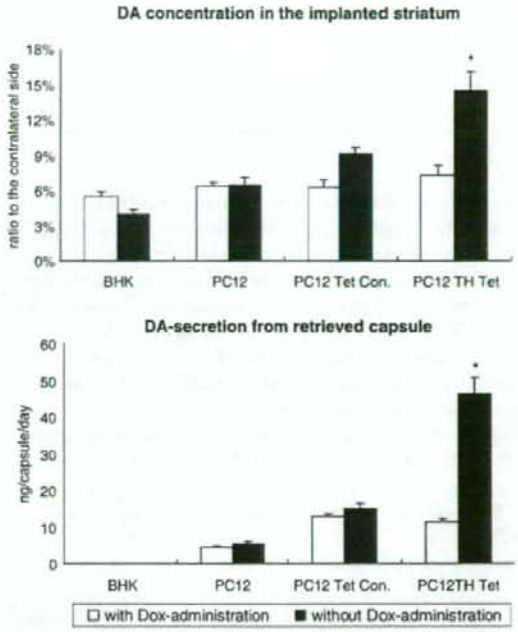


**Fig. 7 – DA concentration in the lesioned and implanted striatum of rats receiving encapsulated cell transplantation and DA-secretion from the retrieved capsule with or without 2-week Dox-administration. Upper: The striatum was punched out at 7 weeks post-implantation or at 9 weeks with washout of Dox for 2 weeks. The percentages of DA concentration in the lesioned and implanted striatum to the non-lesioned striatum demonstrated that DA concentration in the striatum of rats euthanized at 9 weeks post-implantation was significantly higher than that obtained at 7 weeks post-implantation. Data are shown as mean values ± SE expressed as percentages of the contralateral side. PC12 Tet Con.; PC12 Tet-Off Control cells. $n = 4$ in each PC12TH Tet-Off and PC12 Tet-Off Control groups, $n = 3$ in each PC12 and BHK groups. *$P$'s $< 0.01$ vs. DA concentration with Dox-administration. Lower: Measurement of DA from the retrieved capsule at 7 weeks post-implantation or at 9 weeks with washout of Dox for 2 weeks was performed by using HPLC. DA-secretion from the retrieved encapsulated PC12TH Tet-Off cells with 2-week washout of Dox was significantly higher than that with 2-week Dox-administration. Data are shown as mean values ± SE expressed as ng/capsule/day. $n = 6$ in PC12TH Tet-Off and PC12 Tet-Off Control groups, $n = 4$ in PC12 and BHK groups. *$P$'s $< 0.01$ vs. DA-secretion from encapsulated cells with Dox-administration.**

with Dox-administration, although the degree of changeover of DA-secretion with or without Dox-administration diminished. The reduction ratio of DA concentration in the CSF from 5 to 7 weeks post-implantation with the second Dox-administration was significantly lower than the ratio from 1 to 3 weeks with the first Dox-administration (22.2 ± 4.6 and 8.3 ± 7.3%, respectively). DA concentration in the CSF of rats receiving the 3 other kinds of capsules exhibited no significant changes with or without Dox-administration.

2.2.3. *Behavioral analysis*

As shown in Fig. 4 right, in rats receiving the PC12TH Tet-Off capsule, the number of apomorphine-induced rotations was 92 ± 8.1 and 98 ± 9.0% of the level before capsule implantation at 1 and 2 weeks during the first Dox-administration, showing significant differences with those without Dox-administration, 69 ± 12 and 67 ± 13%. Two-week discontinuation of Dox-administration reduced the rotation number to 51 ± 10%, significantly lower than that before Dox-administration (Fig. 6: PC12TH Tet-Off; $F_{7,104} = 4.1$, $P = 0.0006$). The second Dox-administration for 1 and 2 weeks apparently increased the rotation number to 91 ± 8.9 and 97 ± 10.3% (at 6 and 7 weeks after capsule implantation). The rotation number was not affected by Dox-administration in rats receiving the other 3 kinds of capsules.

2.2.4. *DA concentration in the implanted striatum and from the retrieved capsule*

DA concentration in the striatum of the intact or lesioned side was 107.4 ± 4.0 or 6.1 ± 0.5 pg/mm$^3$, showing a significant reduction to 5.6% of the intact side. The percentages of DA concentration in the implanted striatum of rats receiving PC12TH Tet-Off cells to the intact side at 7 weeks (in off-state with Dox-administration) or 9 weeks (in on-state without Dox-administration) post-implantation are shown in Fig. 7. The percentages of DA concentration with or without Dox-administration were 7.3 ± 0.9 or 14.5 ± 1.6% of the intact side. The percentages of DA concentration in the striatum of rats receiving the other 3 kinds of capsule showed no apparent differences with or without Dox-administration, although those with PC12 Tet-Off Control capsule displayed a little significant differences ($P = 0.04$). DA-secretion from the retrieved capsule with or without Dox-administration was 11.2 ± 1.2 or 46.2 ± 4.4 ng/capsule/day (Fig. 7). DA-secretion from the other 3 kinds of capsule did not alter with or without Dox-administration.

2.2.5. *Capsule analysis and immunohistochemistry*

All the grafted capsules were located within the striatum and contiguous to host tissue. Hematoxylin and eosin staining of the capsules retrieved from the brain at 7 or 9 weeks post-implantation showed that PC12TH Tet-Off cells survived in the capsule (Fig. 8). Hematoxylin and eosin staining of the brain also demonstrated that the host response to the capsule was minimal, in accordance with what has been described previously (Yoshida et al., 2003). Each section of the brain was examined by TH staining to analyze the TH positive fibers in the striatum and the TH positive neurons in the SNc, revealing that the fibers and neurons degenerated to almost the same degree, that is, about 14 and 5% of the intact side of

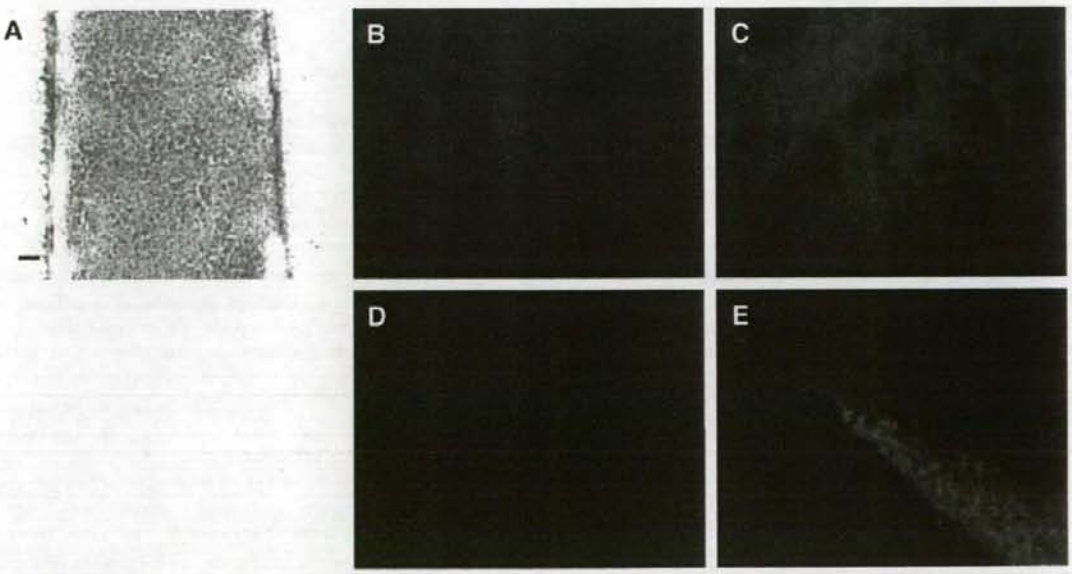


**Fig. 8 – Hematoxylin and eosin staining of the retrieved capsule and TH staining of the striatum and the SNc of rats. Hematoxylin and eosin staining of the retrieved capsule showed many surviving cells at the end of in vivo experiment regardless of the Dox-administration (A). TH staining of the striatum of implanted (after 6-OHDA lesioned) side revealed almost no surviving DA fibers in the striatum (B), compared to that of the intact side (C), displaying well stained DA fibers. Similarly, the number of DA neurons remarkably decreased in the lesioned SNc (D), compared to that in the intact SNc (E). Scale bar = 40 μm (A–C), 100 μm (D, E).**

TH positive fibers in the striatum and TH positive neurons in the SNc were preserved, regardless of the kind of implanted capsule (Fig. 8).

## 3. Discussion

In the present study, we investigated TH-expression controlled by Dox-administration with subsequent DA-secretion by encapsulated cell transplantation. The measurement of DA and RT-PCR revealed that TH-expression could be controlled by Dox-administration in vitro, thus indicating a capacity for dynamic changeover of TH-expression in vivo. Then in an in vivo study, DA concentration in the CSF and the apomorphine-induced rotations revealed that Dox-administration decreased DA-secretion in the rats receiving the PC12TH Tet-Off capsule with a deterioration of the control as time advanced. On the other hand, the amount of DA in the striatum and from the retrieved capsule was found to be dependent on Dox-administration. These results demonstrated that TH-expression with subsequent DA-secretion was well controlled by Dox-administration in vitro for 3 months and partially controlled in vivo for 7 weeks with waning control of DA-secretion.

### 3.1. *Tet-Off system*

Dox-controlled expression of hTH using adenovirus was reported by Corti et al. (1999). An adenovirus vector encoding hTH with Tet-Off system was directly injected into the DA depleted striatum of a rat model of PD, followed by the estimation of TH-expression (Corti et al., 1999). Compared to the study, we used an encapsulation technique for enjoying advantages without direct viral injection. Serial measurements of DA concentration in the CSF by HPLC and behavioral investigations in the course of changeover of Dox-administration every 2 weeks revealed that effective control of DA-secretion from the capsule might be achieved mainly owing to good control of TH-expression. Furthermore, at the end of the study, DA concentration in the striatum and from the capsule apparently showed long-term control of TH-expression with or without Dox-administration.

Successful control of transgene expression would be ideal for certain therapeutic targets, especially in consideration of the needs of clinical applications. Tet-Off system is thought to provide for sharp changeover in the expression of genes. Tet-Off system with an adenovirus vector can provide negative control of gene expression ranging from 20 to 500-fold, although Tet-On system was shown to increase gene expression by only 2 to 28-fold and required a much higher concentration of Dox (Mizuguchi and Hayakawa, 2002). On the contrary, the functional stability of Tet-On system for 1 month in vitro and effectiveness in some in vivo studies were confirmed (Fender et al., 2002; Hagihara et al., 1999; Saitoh et al., 1998). The long-term control of gene expression is difficult, although a follow-up for over 30 weeks did reveal the successful control of erythropoietin-secretion from encapsulated myoblasts (Sommer et al., 2002). In our study, the changeover of TH-expression was recognized by using Tet-Off system for 3 months in vitro and 7 weeks in vivo. However, the decrease of the reduction ratio of DA concentration in the CSF should be overcome by newly developed methods for clinical application in the future. Fortunately, more effective transgene expression with Tet-system has been also reported recently. The vector in which transcription of both the reverse Tet transactivator (rtTA) and the transgene was initiated from a bidirectional Tet-responsive promoter was reported to display rapid switch-off (Chtarto et al., 2003). Rapid and stable induction with low doses of Dox was also achieved by using rtTA2S-M2 transactivator and insulator-flanked reporter vectors (Qu et al., 2004). Alternatively, lentivirus vector has been considered as one of hopeful candidates for clinical application because the safety improved remarkably with the generation of self-inactivating vectors and a minimal packaging system (Miyoshi et al., 1998). Tet-controlled gene expression with lentivirus has been also reported increasingly (Kafri et al., 2000; Regulier et al., 2002; Vogel et al., 2004).

### 3.2. *CSF sampling and DA concentration*

Sampling of the CSF was performed every week for 8 weeks in our study. A 27-gauge needle was used for manual centesis of the cisterna magna. The neck of the sampled rats was flexed adequately. Various techniques are reported on the CSF sampling (De la Calle and Paino, 2002; Espino et al., 1995; Frankmann, 1986; Huang et al., 1996; Hudson et al., 1994; Lai et al., 1983). For repeated CSF sampling, some authors use a catheter placed in the cisterna magna of anesthetized rats (Frankmann, 1986; Lai et al., 1983), although in our study, repetitive centeses under general anesthesia were performed every week in order to minimalize the risk of inflammation and infection. The position of rats, the depth, and angle of the inserted needle and the recognition of a perforation of the dura mater were all important for appropriate CSF sampling (Huang et al., 1996; Hudson et al., 1994).

DA concentration of 6-OHDA lesioned striatum and the CSF has also been examined by certain other authors (Ben et al., 1999; Espino et al., 1995; Teicher et al., 1998; van der Vegt et al., 2003). The data in our study are essentially in correlation with these previously reported findings. However, it is difficult to determine how much DA increase by encapsulated cell implant was adequate for functional recovery or to know how DA concentration in the CSF corresponded to the local DA concentration in the striatum. Serial measurement of DA in the CSF is very useful but at the same time we should be aware of the limitation of this estimation.

Previous studies using either ex vivo approaches or viral vectors for local delivery of LD in the brain have demonstrated that the co-factor biopterin or the rate-limiting enzyme in the biopterin synthesis, GTP-cyclohydrolase-1, needs to be supplied for efficient LD production in addition to TH (Bencsics et al., 1996; Kirik et al., 2002; Leff et al., 1998). In our study, LD production of PC12 cells increased about 5-fold with human TH gene transfection. At least endogenous biopterin from PC12 cells has a capacity of responding to increased TH, although co-transfection with biopterin might increase LD production.

### 3.3. Dyskinetic side effects of DRT

Recent studies clarified that LD might slow the progression of PD rather than hasten at least symptomatically (Fahn and The Parkison Study Group, 2005; The Parkinson Study Group, 2004), although LD has the neurotoxic properties by producing reactive oxygen (Fahn, 1996). The studies also demonstrated that levodopa, especially with high dose, causes various side effects, including dyskinesia, and thus the authors recommended tailor-made medication for each patient in consideration of the clinical responses and side effects (The Parkinson Study Group, 2004). LD-induced dyskinesia was caused by repeated DRT and once dyskinesia has been established, the dyskinetic movements get worse and worse and sometimes resistant to therapy including discontinuation of DRT (Brotchie, 2005), although recently surgical treatments, such as bilateral stimulation of subthalamic nucleus (Schupbach et al., 2005), bilateral subthalamotomy (Alvarez et al., 2005), or pallidotomy (Vitek et al., 2003) were reported as an effective answer to dyskinesia. On the other hand, continuous LD administration using daytime intraintestinal infusion was associated with reduced motor complications including dyskinesia (Stocchi et al., 2005). With our encapsulation technique, patients suffering from dyskinesia might benefit from the continuous and local LD administration. Furthermore, Tet-Off system might contribute to the reduced dyskinesia in the future, although the quick changeover of DA-secretion with much titration of Dox doses should be achieved.

### 3.4. Encapsulation technique

Two decades ago, the efficacy of PC12 cell transplantation for Parkinson's disease model animal was clarified (Freed et al., 1986; Hefti et al., 1985). However, it needed some devices to prevent from immunological rejection as a xenogeneic graft and subsequently studies of encapsulated cell transplantation using PC12 cells arose (Aebischer et al., 1991; Emerich et al., 1993; Kordower et al., 1995). Encapsulated cell transplantation has been used in certain diseases of the central nervous system, including chronic pain (Buchser et al., 1996), amyotrophic lateral sclerosis (Aebischer et al., 1996), Huntington's disease (Bachoud-Levi et al., 2000), and PD (Date et al., 1995). Problems accompanying cell transplantation like tumorigenesis and immunological rejection should be preventable by using this technique. The elimination of systemic side effects of DRT is one of the advantages. Furthermore, the encapsulated cell transplantation has still other merits. The method would enable the delivery of a continuous and stable dose administration of various factors such as GDNF and VEGF (Date et al., 2000; Yasuhara et al., 2004; Yasuhara et al., 2005a, b). Besides, the damage to transplanted cells inside capsule during surgical procedure might be far less than cell transplantation using a single cell solution, because cells inside the hard envelope did not receive any shear force. Subsequently, good survival of transplanted cells inside capsule was achieved for over 3 months (over 70%). In addition to a powerful method relevant to clinical applications, encapsulated cell transplantation has also an important role to play in neural stem cell research. The percentages of neuronal differentiation from the transplanted neural stem cells are very small to date (Chu et al., 2004), although the replacement and re-innervation derived from neural stem cells are idealistic. Comparative study of neural stem cell transplantation with or without encapsulation technique might clarify the contribution of trophic factors secreted from transplanted cells (Jung et al., 2004; Lu et al., 2003), demonstrating the reason of discrepancy between functional recovery and the surviving rate of transplanted cells (Ourednik et al., 2002). Furthermore, selective differentiation of neural progenitor cell was achieved by high-epitope density nanofibers (Silva et al., 2004), thus suggesting the potential of using the capsule as a scafford for neuronal differentiation.

## 4. Conclusion

In conclusion, TH-expression and DA-secretion of PC12TH Tet-Off cells were controllable by Dox-administration in vitro. In addition, serial estimation of drug-induced rotations and DA concentration in the CSF was performed in a rat model of Parkinson's disease. DA-secretion might be partially controlled by Dox-administration for 7 weeks in vivo. However, the reduction ratio of DA concentration in the CSF from 5 to 7 weeks post-implantation with Dox-administration was significantly lower than the ratio from 1 to 3 weeks, suggesting that Tet-Off system used in this study had limitations and that we should explore a more efficient way to control DA-secretion. In the future, this system and concept might help patients with drug-induced dyskinesia by allowing a precise determination of the appropriate doses of drug in the brain, although quicker regulation of DA-secretion and much titration of dose of this system should also be explored, in addition to pre-clinical toxicology and safety studies.

## 5. Experimental procedures

### 5.1. Dox-controlled TH-expression in vitro

#### 5.1.1. PC12TH Tet-Off cell line production

The vector pBluescriptKS(-)hTH1 (Imaoka et al., 1998) was digested at the *Bam*HI and *Cla*I sites and a hTH1 cDNA fragment was introduced into the *Bam*HI and *Cla*I sites of the pTRE2hyg vector (BD Biosciences, CA, U.S.A.), a plasmid containing the Tet Responsive Element (TRE), $P_{minCMV}$, that promotes the expression of genes downstream, and the hygromycin resistance gene, resulting in pTRE2hygTH1. Then the pTRE2hygTH1 construct was transfected into PC12 Tet-Off cells (BD Biosciences), containing tetracycline transactivator (tTA) gene under the control of TetO promoter, using a cationic liposome (Lipofectamin™ 2000; Invitrogen, CA, U.S.A.) mediated DNA delivery method. The transfected PC12TH Tet-Off cells or PC12 Tet-Off cells transfected by the expression vector without hTH cDNA (PC12 Tet-Off Control) were grown in Eagle's DMEM (EMEM) supplemented with 10% horse serum, 10% fetal bovine serum, and antibiotic solution at 37 °C in a 10% $CO_2$/90% air humidified atmosphere. The transfected cells were selected in 250 μg/ml of G418 (WAKO, Japan) and HygromycinB (WAKO, Japan) to amplify the copy number of

the integrated plasmid. Four weeks later, drug-resistant colonies were visualized and picked up as the cell clones. Eighty clones were selected and the amount of levodopa (LD) and DA-secretion was measured with HPLC-ECD (Shiseido, Osaka, Japan). The characteristics of the cell clone were then confirmed for the expression of hTH and tTA with reverse transcription-polymerase chain reaction (RT-PCR). Cell clone number E6, secreting a sufficient amount of both LD and DA with optimal negative control of TH-expression and DA-secretion with Dox-administration (Sigma, St. Louis, MO) was used in the following study. For up to 3 months after culturing, the reduction of TH-expression and DA-secretion was achieved by Dox-administration in vitro.

#### 5.1.2. RT-PCR

Total RNA was isolated from $1 \times 10^6$ cells of PC12TH Tet-Off or PC12 Tet-Off Control cells cultured with or without Dox and used directly for the first-strand cDNA synthesis. RT was performed with a superscript III First-Strand Synthesis system for PCR (Invitrogen, CA, U.S.A.). PCR was conducted as follows: 10% of the RT product was mixed with 0.2 mM dNTPs, 0.2 mM $MgCl_2$, 10 pM of each primer, and 2 units of Taq polymerase (Invitrogen) in a final volume of 20 μl. The conditions for the amplification cycles were: denaturing at 94 °C for 30 s, annealing at 65 °C for 30 s, and extending at 72 °C for 1 min with 30 cycles of amplification. The primers used for amplification were as follows: hTH; 5′-CGGTGGAGTTCGGGCTGTG-TAAG-3′ (sense) and 5′-CACAACCTCACCACGGGCACAC-3′ (antisense) tTA; 5′-CAACCCGTAAACTCGCCCAGAAG-3′ (sense) and 5′-GCAACCTAAAGTAAAATGCCCCACAG-3′ (antisense). The sense and antisense for hTH cDNA were designed to distinguish from rat TH derived from PC12 Tet-Off cells. Sense and antisense were synthesized and purified at Sigma Genosys Japan (Hokkaido, Japan). A total of 10 μl of final PCR product was separated in a 2.0% agarose gel, stained with ethidium bromide, and photographed.

#### 5.1.3. *Cell culture, Dox-administration, and HPLC-ECD analysis*

We used baby hamster kidney (BHK) cells (JRCB, Osaka, Japan), PC12 Tet-Off Control cells, and PC12 cells (clone B3) provided by Drs. Masami Takahashi and Yoko Shoji-Kasai (Life Science Research Center, Mitsubishi Chemicals, Tokyo, Japan), who had subIcloned them (Shoji-Kasai et al., 1992), as controls for all experiments. We cultured PC12TH Tet-Off cells and PC12 Tet-Off Control cells in culture medium supplemented with 250 μg/ml of HygromycinB and G418, while PC12 cells and BHK cells were cultured in culture medium without these anticancer drugs. The amount of catecholamine-secretion was measured in plain EMEM obtained from these cultured cells incubated for 2 h and converted to the daily amount.

First, in order to determine the appropriate dose of Dox with which the TH-expression of PC12TH Tet-Off cells could be controlled, we measured the amount of catecholamine-secretion in EMEM obtained from cultured $1 \times 10^6$ cells incubated for 2 h after 7 day-treatment of 0, 10, 50, 100, 200, 500, and 1000 ng/ml of Dox. Each cultured medium with or without Dox was exchanged every other day for the week ($n = 5$ in each group). Each sample was assayed using HPLC-ECD to measure the amount of catecholamine, as previously described (Yoshida et al., 2003). The mobile phase consisted of 100 mM potassium dihydrogen phosphate, 50 mM sodium acetate, 1.3 mM phosphoric acid, 0.7 mM octanesulfonic acid, 0.27 mM EDTA, and 5% acetonitrile at pH 2.7, filtered with a 0.2 mm pore-sized filter.

#### 5.1.4. *Encapsulation*

Polymeric hollow fibers consisting of semipermeable membrane (Amicon, MA, U.S.A.) were used as capsules. They are made of polysulfone (molecular cut-off: 100 kDa) and exhibit a cross-sectional inner diameter 700 μm. Devices 7.0 mm in length were sealed at the distal end prior to cell loading with light-cured dental cement (PALFIQUE CLEAR®, Tokuyama Dental Corp., Tokyo, Japan). PC12TH Tet-Off, PC12 Tet-Off Control, PC12 cells, or BHK cells were prepared as a single cell suspension and loaded from the proximal end at a density of $1 \times 10^6$ cells/capsule. The access port was also sealed with light cured dental cement. Four kinds of encapsulated cells were cultured into 12 well culture plates and maintained in EMEM containing 10% horse serum and 10% fetal bovine serum. After 2 weeks in culture, 100 ng/ml of Dox-administration for 2 weeks was started. Culture medium with Dox was exchanged every other day. Two weeks later, Dox-administration was discontinued, following this changeover of 2-week Dox-administration and discontinuation for over 70 days. Three, 7, 14, 17, 21, 28, 31, 35, 42, 45, 49, 56, 59, 63, and 70 days after the beginning of the first Dox-administration, the capsules were rinsed in EMEM and placed in 1 ml fresh EMEM for 2 h to be analyzed for HPLC ($n = 6$ in each group).

### 5.2. *Control of TH-expression with Dox-administration in a rat model of PD*

#### 5.2.1. *Test animals*

We used adult female Sprague–Dawley rats ($n = 60$, 200–250 g at the beginning of the experiment, Charles River, Japan) according to the approved guidelines of the institutional animal care and use committee of Okayama University. They were housed in pairs per cage in a temperature and humidity controlled room that was maintained on a 12 h light: dark cycle, and they had free access to food and water with or without Dox.

#### 5.2.2. *Surgical procedures*

All rats were deeply anesthetized with sodium pentobarbital (30 mg/kg, i.p.) and placed in a stereotaxic instrument (Narishige, Japan). A midline skin incision was made in the skull, and a burr hole was drilled. With pre-treatment of desipramin (25 mg/kg, i.p., Sigma), 5 and 7.5 μg of 6-hydroxydopamine (6-OHDA; 1 and 1.5 μl of 5 μg/μl dissolved in saline containing 0.2 mg/ml ascorbic acid; Sigma) were injected into the right medial forebrain bundle (MFB) and the right substantia nigra pars compacta (SNc) with a 28-gauge Hamilton syringe at the following 2 coordinates: [4.2, 1.6, 7.8] and [4.8, 1.8, 7.5]; [X mm posterior to the bregma, Y mm right to the sagittal suture, and Z mm ventral to the surface of the brain] with the height of the lambda at the same level as the bregma (Paxinos, 1998). The injection rate was 1 μl/min, and the syringe was left in place for an additional 5 min before

being retracted slowly (1 mm/min). One month after lesioning, an apomorphine-induced rotational test was performed and rats of which the number of rotations exceeded 5 turns/min for 1 h on average were used for this study. A single capsule containing PC12TH Tet-Off ($n$ = 26), PC12 Tet-Off Control ($n$ = 14), PC12 ($n$ = 10), or BHK cells ($n$ = 10) was unilaterally implanted in the right striatum of the rats. The stereotaxic coordinates for the capsule graft were [0.0, 3.0, 6.5] with the tooth-bar set at 0.0 mm. At the end of the experiment, 20 rats received a skin incision over the implantation site under anesthesia with sodium pentobarbital (30 mg/kg, i.p.). Then the dura mater of all rats was cut to expose the capsule and it was retrieved from brain. The explanted capsules were rinsed in EMEM and placed in 1 ml of EMEM for 2 h and the supernatant was analyzed using HPLC. Half of the rats were sacrificed for histological examination.

#### 5.2.3. *Dox-administration and sampling of the CSF and the striatum*

In order to switch off TH-expression and DA-secretion, we dissolved Dox in the animals' drinking water to a final concentration of 0.5 mg/ml supplemented with 2.5% sucrose after the dose had been determined in preliminary studies. Dox-administration was started 1 week after capsule implantation. We replenished the drinking water three times per week. First, rats receiving PC12TH Tet-Off capsule were divided into 2 groups ($n$ = 6 in each), that is, with or without Dox-administration, following 2-week estimation of DA concentration in the CSF and the number of apomorphine-induced rotations. Next, the changeover of 2-week Dox-administration and discontinuation was continued for over 70 days using rats implanted PC12TH Tet-Off ($n$ = 14), PC12Tet-Off Control ($n$ = 14), PC12 ($n$ = 10), and BHK capsule ($n$ = 10). Every week, we collected 50–100 μl of cerebrospinal fluid (CSF) from the cisterna magna with a 27-gauge needle for catecholamine measurement by HPLC under anesthesia with sodium pentobarbital (30 mg/kg, i.p.). CSF samples were filtered with SLGV R04 NL filters (0.22 μm pore size, Millipore) and 50 μl was used for HPLC analysis ($n$ = 8 in PC12TH Tet-Off and PC12Tet-Off groups and $n$ = 5 in PC12 and BHK groups). At 7 weeks after implantation, half of the rats were euthanized with overdosed sodium pentobarbital (300 mg/kg, i.p.). The other rats were sacrificed at 2 weeks after discontinuation of Dox-administration. Each brain was quickly removed and then cut into 2 mm-thick sections ($n$ = 6 in PC12TH Tet-Off and PC12Tet-Off Control groups and $n$ = 4 in PC12 and BHK groups with or without Dox-administration). A section at +0.0 mm anterior to the bregma was selected and 2 small pieces of tissue in each hemisphere were punched out. The tissue sample (about 14 $mm^3$) was homogenized by sonication in 200 μl of 0.1 M $HClO_4$. The homogenates were centrifuged for 5 min (13,500 rpm) and 50 μl of the supernatant was used for HPLC analysis.

#### 5.2.4. *Behavioral testing*

Rats were challenged with apomorphine (0.3 mg/kg, s.c., Sigma) before implantation for the confirmation of PD model and weekly after implantation. Rotational behaviors were assessed for 60 min with a video camera. Full 360° turns in the direction contralateral to the lesion were counted.

#### 5.2.5. *Fixation and sectioning*

At 8 weeks after implantation, 10 rats were perfused through the ascending aorta with 200 ml of cold PBS, followed by 100 ml of 4% PFA in PBS under deep anesthesia. Brains were removed and post-fixed in the same fixative for 3 days followed by 30% sucrose in phosphate buffer (PB) for 1 week. Six series of coronal sections were cut at a thickness of 40 μm in a freezing microtome and stored at −20 °C.

#### 5.2.6. *Capsule analysis*

After retrieval and HPLC analysis, all encapsulated PC12TH Tet-Off, PC12 Tet-Off Control, PC12, and BHK cells were frozen with O.C.T. compound (Tissue-Tek, U.S.A), after removing the attached tissue from the capsule wall and washing with plain DMEM. Specimens were cut in longitudinal sections of 20 μm and stained with hematoxylin and eosin.

#### 5.2.7. *Immunohistochemistry*

Free floating sections for immunohistochemistry were incubated overnight at 4 °C with anti-TH antibody (rabbit polyclonal, 1:1000, Chemicon) and 10% normal goat serum. After several rinses in PBS, sections were incubated for 1 h in anti-rabbit IgG Cy3 conjugate (1:1000, sigma) as a secondary antibody, mounted on albumin-coated slides and sealed. Control studies included exclusion of primary antibody substituted with 10% normal goat serum in PBS. No immunoreactivity was observed in these controls.

#### 5.2.8. *Statistical analysis*

Data were evaluated statistically using one way ANOVA followed by post hoc Scheffe's test or Mann–Whitney's $U$ test for the small sample size and the statistical comparisons are shown by Mann–Whitney's $U$ test unless specified otherwise. Statistical significance was preset at $P < 0.05$.

## Acknowledgments

We thank Drs. Masami Takahashi and Yoko Shoji-Kasai (Life Science Research Center, Mitsubishi Chemicals, Tokyo, Japan) for giving us PC12 cells (clone B3), Hideki Wakimoto for photographic work, Masako Arao and Tomoko Ujibashi for technical assistance. This work was supported in part by Grants-in-Aid for Scientific Research and the Grant of the project for realization of regenerative medicine from the Ministry of Education, Culture, Sports, Science and Technology in Japan.

## REFERENCES

Aebischer, P., Tresco, P.A., Winn, S.R., Greene, L.A., Jaeger, C.B., 1991. Long-term cross-species brain transplantation of a polymer-encapsulated dopamine-secreting cell line. Exp. Neurol. 111, 269–275.

Aebischer, P., Pochon, N.A., Heyd, B., Deglon, N., Joseph, J.M., Zurn, A.D., Baetge, E.E., Hammang, J.P., Goddard, M., Lysaght, M., Kaplan, F., Kato, A.C., Schluep, M., Hirt, L., Regli, F., Porchet, F., De Tribolet, N., 1996. Gene therapy for amyotrophic lateral sclerosis (ALS) using a polymer encapsulated xenogenic cell line engineered to secrete hCNTF. Hum. Gene Ther. 7, 851–860.

Alvarez, L., Macias, R., Lopez, G., Alvarez, E., Pavon, N., Rodriguez-Oroz, M.C., Juncos, J.L., Maragoto, C., Guridi, J., Litvan, I., Tolosa, E.S., Koller, W., Vitek, J., DeLong, M.R., Obeso, J.A., 2005. Bilateral subthalamotomy in Parkinson's disease: initial and long-term response. Brain 128, 570–583.

Bachoud-Levi, A.C., Deglon, N., Nguyen, J.P., Bloch, J., Bourdet, C., Winkel, L., Remy, P., Goddard, M., Lefaucheur, J.P., Brugieres, P., Baudic, S., Cesaro, P., Peschanski, M., Aebischer, P., 2000. Neuroprotective gene therapy for Huntington's disease using a polymer encapsulated BHK cell line engineered to secrete human CNTF. Hum. Gene Ther. 11, 1723–1729.

Ben, V., Blin, O., Bruguerolle, B., 1999. Time-dependent striatal dopamine depletion after injection of 6-hydroxydopamine in the rat. Comparison of single bilateral and double bilateral lesions. J. Pharm. Pharmacol. 51, 1405–1408.

Bencsics, C., Wachtel, S.R., Milstien, S., Hatakeyama, K., Becker, J.B., Kang, U.J., 1996. Double transduction with GTP cyclohydrolase I and tyrosine hydroxylase is necessary for spontaneous synthesis of L-DOPA by primary fibroblasts. J. Neurosci. 16, 4449–4456.

Bondanza, A., Ciceri, F., Bonini, C., 2005. Application of donor lymphocytes expressing a suicide gene for early GVL induction and later control of GVH reactions after bone-marrow transplantation. Methods Mol. Med. 109, 475–486.

Brotchie, J.M., 2005. Nondopaminergic mechanisms in levodopa-induced dyskinesia. Mov. Disord. 20, 919–931.

Buchser, E., Goddard, M., Heyd, B., Joseph, J.M., Favre, J., de Tribolet, N., Lysaght, M., Aebischer, P., 1996. Immunoisolated xenogenic chromaffin cell therapy for chronic pain. Initial clinical experience. Anesthesiology 85, 1005–1012 (discussion 29A-30A).

Chtarto, A., Bender, H.U., Hanemann, C.O., Kemp, T., Lehtonen, E., Levivier, M., Brotchi, J., Velu, T., Tenenbaum, L., 2003. Tetracycline-inducible transgene expression mediated by a single AAV vector. Gene Ther. 10, 84–94.

Chu, K., Kim, M., Park, K.I., Jeong, S.W., Park, H.K., Jung, K.H., Lee, S. T., Kang, L., Lee, K., Park, D.K., Kim, S.U., Roh, J.K., 2004. Human neural stem cells improve sensorimotor deficits in the adult rat brain with experimental focal ischemia. Brain Res. 1016, 145–153.

Corti, O., Sanchez-Capelo, A., Colin, P., Hanoun, N., Hamon, M., Mallet, J., 1999. Long-term doxycycline-controlled expression of human tyrosine hydroxylase after direct adenovirus-mediated gene transfer to a rat model of Parkinson's disease. Proc. Natl. Acad. Sci. U. S. A. 96, 12120–12125.

Date, I., Asari, S., Ohmoto, T., 1995. Two-year follow-up study of a patient with Parkinson's disease and severe motor fluctuations treated by co-grafts of adrenal medulla and peripheral nerve into bilateral caudate nuclei: case report. Neurosurgery 37, 515–518 (discussion 518-9).

Date, I., Shingo, T., Yoshida, H., Fujiwara, K., Kobayashi, K., Ohmoto, T., 2000. Grafting of encapsulated dopamine-secreting cells in Parkinson's disease: long-term primate study. Cell Transplant 9, 705–709.

Dawson, T.M., Dawson, V.L., 2002. Neuroprotective and neurorestorative strategies for Parkinson's disease. Nat. Neurosci. 5, 1058–1061 (Suppl).

De la Calle, J.L., Paino, C.L., 2002. A procedure for direct lumbar puncture in rats. Brain Res. Bull. 59, 245–250.

Emerich, D.F., McDermott, P.E., Krueger, P.M., Frydel, B., Sanberg, P.R., Winn, S.R., 1993. Polymer-encapsulated PC12 cells promote recovery of motor function in aged rats. Exp. Neurol. 122, 37–47.

Espino, A., Llorens, J., Calopa, M., Bartrons, R., Rodriguez-Farre, E., Ambrosio, S., 1995. Cerebrospinal dopamine metabolites in rats after intrastriatal administration of 6-hydroxydopamine or 1-methyl-4-phenylpyridinium ion. Brain Res. 669, 19–25.

Fahn, S., 1996. Is levodopa toxic? Neurology 47 (suppl. 3), S184–S195.

Fahn, S., The Parkinson Study Group, 2005. Does levodopa slow or hasten the rate of progression of Parkinson's disease? J. Neurol. 252 (Suppl. 4), iv37–iv42.

Fender, P., Jeanson, L., Ivanov, M.A., Colin, P., Mallet, J., Dedieu, J.F., Latta-Mahieu, M., 2002. Controlled transgene expression by E1-E4-defective adenovirus vectors harbouring a "tet-on" switch system. J. Gene Med. 4, 668–675.

Frankmann, S.P., 1986. A technique for repeated sampling of CSF from the anesthetized rat. Physiol. Behav. 37, 489–493.

Freed, W.J., Patel-Vaidya, U., Geller, H.M., 1986. Properties of PC12 pheochromocytoma cells transplanted to the adult rat brain. Exp. Brain Res. 63, 557–566.

Freed, C.R., Greene, P.E., Breeze, R.E., Tsai, W.Y., DuMouchel, W., Kao, R., Dillon, S., Winfield, H., Culver, S., Trojanowski, J.Q., Eidelberg, D., Fahn, S., 2001. Transplantation of embryonic dopamine neurons for severe Parkinson's disease. N. Engl. J. Med. 344, 710–719.

Hagihara, Y., Saitoh, Y., Arita, N., Eguchi, Y., Tsujimoto, Y., Yoshimine, T., Hayakawa, T., 1999. Long-term functional assessment of encapsulated cells transfected with Tet-On system. Cell Transplant 8, 431–434.

Hefti, F., Hartikka, J., Schlumpf, M., 1985. Implantation of PC12 cells into the corpus striatum of rats with lesions of the dopaminergic nigrostriatal neurons. Brain Res. 348, 283–288.

Huang, Y.L., Saljo, A., Suneson, A., Hansson, H.A., 1996. Comparison among different approaches for sampling cerebrospinal fluid in rats. Brain Res. Bull. 41, 273–279.

Hudson, L.C., Hughes, C.S., Bold-Fletcher, N.O., Vaden, S.L., 1994. Cerebrospinal fluid collection in rats: modification of a previous technique. Lab. Anim. Sci. 44, 358–361.

Imaoka, T., Date, I., Ohmoto, T., Nagatsu, T., 1998. Significant behavioral recovery in Parkinson's disease model by direct intracerebral gene transfer using continuous injection of a plasmid DNA-liposome complex. Hum. Gene Ther. 9, 1093–1102.

Jung, C.G., Hida, H., Nakahira, K., Ikenaka, K., Kim, H.J., Nishino, H., 2004. Pleiotrophin mRNA is highly expressed in neural stem (progenitor) cells of mouse ventral mesencephalon and the product promotes production of dopaminergic neurons from embryonic stem cell-derived nestin-positive cells. FASEB J. 18, 1237–1239.

Kafri, T., van Praag, H., Gage, F.H., Verma, I.M., 2000. Lentiviral vectors: regulated gene expression. Mol. Ther. 1, 516–521.

Kirik, D., Georgievska, B., Burger, C., Winkler, C., Muzyczka, N., Mandel, R.J., Bjorklund, A., 2002. Reversal of motor impairments in parkinsonian rats by continuous intrastriatal delivery of L-dopa using rAAV-mediated gene transfer. Proc. Natl. Acad. Sci. U. S. A. 99, 4708–4713.

Kordower, J.H., Liu, Y.T., Winn, S., Emerich, D.F., 1995. Encapsulated PC12 cell transplants into hemiparkinsonian monkeys: a behavioral, neuroanatomical, and neurochemical analysis. Cell Transplant 4, 155–171.

Lai, Y.L., Smith, P.M., Lamm, W.J., Hildebrandt, J., 1983. Sampling and analysis of cerebrospinal fluid for chronic studies in awake rats. J. Appl. Physiol. 54, 1754–1757.

Leff, S.E., Rendahl, K.G., Spratt, S.K., Kang, U.J., Mandel, R.J., 1998. In vivo L-DOPA production by genetically modified primary rat fibroblast or 9 L gliosarcoma cell grafts via coexpression of GTPcyclohydrolase I with tyrosine hydroxylase. Exp. Neurol. 151, 249–264.

Lu, P., Jones, L.L., Snyder, E.Y., Tuszynski, M.H., 2003. Neural stem cells constitutively secrete neurotrophic factors and promote extensive host axonal growth after spinal cord injury. Exp. Neurol. 181, 115–129.

Ma, Y., Feigin, A., Dhawan, V., Fukuda, M., Shi, Q., Greene, P., Breeze, R., Fahn, S., Freed, C., Eidelberg, D., 2002. Dyskinesia

after fetal cell transplantation for parkinsonism: a PET study. Ann. Neurol. 52, 628–634.
Miyoshi, H., Blomer, U., Takahashi, M., Gage, F.H., Verma, I.M., 1998. Development of a self-inactivating lentivirus vector. J. Virol. 72, 8150–8157.
Mizuguchi, H., Hayakawa, T., 2002. The tet-off system is more effective than the tet-on system for regulating transgene expression in a single adenovirus vector. J. Gene Med. 4, 240–247.
Nutt, J.G., Carter, J.H., Lea, E.S., Sexton, G.J., 2002. Evolution of the response to levodopa during the first 4 years of therapy. Ann. Neurol. 51, 686–693.
Olanow, C.W., Goetz, C.G., Kordower, J.H., Stoessl, A.J., Sossi, V., Brin, M.F., Shannon, K.M., Nauert, G.M., Perl, D.P., Godbold, J., Freeman, T.B., 2003. A double-blind controlled trial of bilateral fetal nigral transplantation in Parkinson's disease. Ann. Neurol. 54, 403–414.
Ourednik, J., Ourednik, V., Lynch, W.P., Schachner, M., Snyder, E.Y., 2002. Neural stem cells display an inherent mechanism for rescuing dysfunctional neurons. Nat. Biotechnol. 20, 1103–1110.
Paxinos, G.W.G., 1998. The Rat Brain in Stereotaxic Coordinates. Academic Press, San Diego.
Qu, Z., Thottassery, J.V., Van Ginkel, S., Manuvakhova, M., Westbrook, L., Roland-Lazenby, C., Hays, S., Kern, F.G., 2004. Homogeneity and long-term stability of tetracycline-regulated gene expression with low basal activity by using the rtTA2S-M2 transactivator and insulator-flanked reporter vectors. Gene 327, 61–73.
Rajput, A.H., Fenton, M.E., Di Paolo, T., Sitte, H., Pifl, C., Hornykiewicz, O., 2004. Human brain dopamine metabolism in levodopa-induced dyskinesia and wearing-off. Parkinsonism Relat. Disord. 10, 221–226.
Regulier, E., Pereira de Almeida, L., Sommer, B., Aebischer, P., Deglon, N., 2002. Dose-dependent neuroprotective effect of ciliary neurotrophic factor delivered via tetracycline-regulated lentiviral vectors in the quinolinic acid rat model of Huntington's disease. Hum. Gene Ther. 13, 1981–1990.
Saitoh, Y., Eguchi, Y., Hagihara, Y., Arita, N., Watahiki, M., Tsujimoto, Y., Hayakawa, T., 1998. Dose-dependent doxycycline-mediated adrenocorticotropic hormone secretion from encapsulated Tet-on proopiomelanocortin Neuro2A cells in the subarachnoid space. Hum. Gene Ther. 9, 997–1002.
Schupbach, W.M., Chastan, N., Welter, M.L., Houeto, J.L., Mesnage, V., Bonnet, A.M., Czernecki, V., Maltete, D., Hartmann, A., Mallet, L., Pidoux, B., Dormont, D., Navarro, S., Cornu, P., Mallet, A., Agid, Y., 2005. Stimulation of the subthalamic nucleus in Parkinson's disease: a 5 year follow up. J. Neurol. Neurosurg. Psychiatry 76, 1640–1644.
Shoji-Kasai, Y., Yoshida, A., Sato, K., Hoshino, T., Ogura, A., Kondo, S., Fujimoto, Y., Kuwahara, R., Kato, R., Takahashi, M., 1992. Neurotransmitter release from synaptotagmin-deficient clonal variants of PC12 cells. Science 256, 1821–1823.
Silva, G.A., Czeisler, C., Niece, K.L., Beniash, E., Harrington, D.A., Kessler, J.A., Stupp, S.I., 2004. Selective differentiation of neural progenitor cells by high-epitope density nanofibers. Science 303, 1352–1355.
Sommer, B., Rinsch, C., Payen, E., Dalle, B., Schneider, B., Deglon, N., Henri, A., Beuzard, Y., Aebischer, P., 2002. Long-term doxycycline-regulated secretion of erythropoietin by encapsulated myoblasts. Mol. Ther. 6, 155–161.
Stocchi, F., Vacca, L., Ruggieri, S., Olanow, C.W., 2005. Intermittent vs. continuous levodopa administration in patients with advanced Parkinson disease: a clinical and pharmacokinetic study. Arch. Neurol. 62, 905–910.
Teicher, M.H., Andersen, S.L., Campbell, A., Gelbard, H.A., Baldessarini, R.J., 1998. Progressive accumbens degeneration after neonatal striatal 6-hydroxydopamine in rats. Neurosci. Lett. 247, 99–102.
The Parkinson Study Group, 2004. Levodopa and the progression of Parkinson's disease. N. Engl. J. Med. 351, 2498–2508.
van der Vegt, B.J., Lieuwes, N., Cremers, T.I., de Boer, S.F., Koolhaas, J.M., 2003. Cerebrospinal fluid monoamine and metabolite concentrations and aggression in rats. Horm. Behav. 44, 199–208.
Vitek, JL., Bakay, R.A., Freeman, A., Evatt, M., Green, J., McDonald, W., Haber, M., Barnhart, H., Wahlay, N., Triche, S., Mewes, K., Chockkan, V., Zhang, J.Y., DeLong, M.R., 2003. Randomized trial of pallidotomy versus medical therapy for Parkinson's disease. Ann. Neurol. 53, 558–569.
Vogel, R., Amar, L., Thi, A.D., Saillour, P., Mallet, J., 2004. A single lentivirus vector mediates doxycycline-regulated expression of transgenes in the brain. Hum. Gene Ther. 15, 157–165.
Yasuhara, T., Shingo, T., Kobayashi, K., Takeuchi, A., Yano, A., Muraoka, K., Matsui, T., Miyoshi, Y., Hamada, H., Date, I., 2004. Neuroprotective effects of vascular endothelial growth factor (VEGF) upon dopaminergic neurons in a rat model of Parkinson's disease. Eur. J. Neurosci. 19, 1494–1504.
Yasuhara, T., Shingo, T., Muraoka, K., Kobayashi, K., Takeuchi, A., Yano, A., Wenji, Y., Kameda, M., Matsui, T., Miyoshi, Y., Date, I., 2005a. Early transplantation of an encapsulated glial cell line-derived neurotrophic factor-producing cell demonstrating strong neuroprotective effects in a rat model of Parkinson disease. J. Neurosurg. 102, 80–89.
Yasuhara, T., Shingo, T., Muraoka, K., wen Ji, Y., Kameda, M., Takeuchi, A., Yano, A., Nishio, S., Matsui, T., Miyoshi, Y., Hamada, H., Date, I., 2005b. The differences between high and low-dose administration of VEGF to dopaminergic neurons of in vitro and in vivo Parkinson's disease model. Brain Res. 1038, 1–10.
Yoshida, H., Date, I., Shingo, T., Fujiwara, K., Kobayashi, K., Miyoshi, Y., Ohmoto, T., 2003. Stereotactic transplantation of a dopamine-producing capsule into the striatum for treatment of Parkinson disease: a preclinical primate study. J. Neurosurg. 98, 874–881.